Psychological Methods

Comparison of Latent Growth Curves: A Parameter Constancy Test

Jesús F. Rosel, Sara Puchol, Marcel Elipe, Patricia Flor, Francisco H. Machancoses, and Juan J. Canales

Online First Publication, November 3, 2025. https://dx.doi.org/10.1037/met0000788

AMERICAN PSYCHOLOGICAL ASSOCIATION

Psychological Methods

ISSN: 1082-989X

https://doi.org/10.1037/met0000788

Comparison of Latent Growth Curves: A Parameter Constancy Test

Jesús F. Rosel[1], Sara Puchol[2], Marcel Elipe[1], Patricia Flor[3], Francisco H. Machancoses[1], and Juan J. Canales[4]

[1] Faculty of Health Sciences, Universidad Jaume I

[2] Independent Researcher, Castellón, Spain

[3] Faculty of Health Sciences, International University of Valencia (VIU)

[4] Faculty of Health and Environmental Sciences, Auckland University of Technology

Abstract

Latent growth curve (LGC) models, implemented through structural equation modeling, are widely used to analyze developmental and learning trajectories. Model selection in LGC often relies on goodness-of-fit indices (e.g., χ^2, Akaike information criterion, and root-mean-square error of approximation), but these metrics fail to assess the temporal constancy, or stability of parameters, an important aspect when forecasting longitudinal data. Addressing this gap, we propose a novel parameter constancy test (PCT) tailored for LGC models. This test evaluates internal constancy, identifies potential breakpoints, helps determine the minimal number of measurement waves needed for reliable modeling, and is also useful for comparing different explanatory models of the analyzed data. To validate this approach, we applied PCT to real-world data, comparing the widely used quadratic function model with the negative exponential model and other nonlinear functions. The results reveal that the negative exponential model, unlike the quadratic function, consistently exhibits parameter constancy even with fewer sampling waves, making it particularly suitable for longitudinal analysis. Additionally, PCT highlights how inappropriate model selection or instability may lead to misinterpretations, particularly in evaluating interventions or extrapolating beyond observed time frames. Our findings emphasize the dual importance of statistical fit and parameter constancy in selecting LGC models. By integrating PCT into standard practice, researchers can better ensure model consistency, optimize resource allocation, and avoid erroneous conclusions in developmental and learning studies.

Translational Abstract

Latent growth curve models are commonly used to track development and learning over time. However, selecting the best model often relies solely on statistical fit indices, which overlook a key factor: whether the model's parameters remain stable across different time points. This stability, or constancy, is critical when models are used to predict immediate or long-term trends or evaluate interventions. To address this issue, we introduce a new parameter constancy test (PCT) specifically for latent growth curve models. PCT not only evaluates whether a model's parameters are consistent across time but also compares models to identify the most reliable option. For example, using PCT, we found that the widely used quadratic function model lacks constancy, whereas the negative exponential model remains consistent even with fewer data points. This means researchers can confidently use fewer measurement waves without sacrificing accuracy. Practically, PCT offers four key benefits: it helps select the best model by estimating more accurate forecast values, detects shifts in data trends, determines the minimal number of data points needed, and reduces resource demands for future studies. By adopting PCT, applied researchers in psychology, education, and health can make more informed decisions, ensuring that their findings are both statistically more adequate and theoretically sounder.

Keywords: latent growth curves, parameter constancy test, structural stability, model comparison, structural equation modeling

Supplemental materials: https://doi.org/10.1037/met0000788.supp

Douglas Steinley served as action editor.

Jesús F. Rosel https://orcid.org/0000-0002-0920-032X

Juan J. Canales https://orcid.org/0000-0003-2884-5227

We thank Terry Jorgensen and Manuel Ato for their help with the syntax of exponential models.

Open Access funding provided by the Auckland University of Technology:

Sara Puchol served as lead for data curation. Patricia Flor contributed equally to visualization. Francisco H. Machancoses served as lead for software. Juan J. Canales contributed equally to supervision. Jesús F. Rosel, Patricia Flor, Francisco H. Machancoses, and Juan J. Canales contributed equally to conceptualization. Jesús F. Rosel, Sara Puchol, Francisco H. Machancoses, and Juan J. Canales contributed equally to writing–original draft. Jesús F. Rosel, Marcel Elipe, and Patricia Flor contributed equally to writing–review and editing. Sara Puchol, Marcel Elipe, Patricia Flor, and Francisco H. Machancoses contributed equally to formal analysis. Jesús F. Rosel, Sara Puchol, Marcel Elipe, and Juan J. Canales contributed equally to methodology.

Correspondence concerning this article should be addressed to Juan J. Canales, Faculty of Health and Environmental Sciences, Auckland University of Technology, AZ Building, 90 Akoranga Drive, Northcote, Auckland 0627, New Zealand. Email: juan.canales@aut.ac.nz

Latent growth curve (LGC) models, implemented through confirmatory factor analysis in structural equation modeling (SEM), have become central to analyzing developmental and learning trajectories. They are widely used to understand growth patterns across time in psychology, education, and health. However, selecting the most suitable model (whether polynomial, nonlinear, or piecewise) remains a complex challenge due to variability in data and theoretical assumptions.

In the field of statistics, tests for structural constancy, or structural stability, and breakpoints are common in cross-sectional and time series data, allowing researchers to detect changes in variable relationships or shifts in the data-generating process (DGP) over time. Yet, in psychological research, particularly in the analysis of LGC, the application of constancy tests is rare. Structural constancy, or inner stability, in a model indicates that relationships between variables remain consistent across different conditions or over time; while breakpoints signal moments where these relationships change significantly, suggesting a shift in the DGP, or structural change. Recognizing these breakpoints can enhance the accuracy and validity of models by revealing when and why a model may no longer fit well, providing insights into underlying changes in the studied phenomena. Traditional SEM fit indices, such as Akaike information criterion (AIC) and root-mean-square error of approximation (RMSEA), assess overall model fit but overlook the temporal constancy of parameters. Parameter constancy test (PCT) addresses this gap by evaluating a model's consistency across different time segments. By combining assessments of fit and constancy, PCT allows researchers to compare models more properly, ensuring the selection of models that remain reliable under varying temporal conditions.

The concept of a DGP is integral to dynamic modeling theory in econometrics (Campos et al., 2005; Florens & Mouchart, 1985; Hendry et al., 1984; Pesaran, 2016). Simply put, a stable DGP ensures that model parameters remain consistent throughout the longitudinal data set. This consistency is essential for reliable forecasting and for distinguishing between genuine developmental changes and model misspecification. Consequently, the model should be capable of projecting into the future, enabling reliable short-, medium-, and long-term forecasts. This aligns with the concept of a long-run trend (LRT), where the model yields credible forecasts over the long term (Campos et al., 2005; Engle & Granger, 1987; Panik, 2014).

This study aims to identify the most suitable LGC models by evaluating both their fit indices and parameter constancy. A PCT provides critical insights into the structural stability of growth models, enabling researchers to identify breakpoints, determine the minimum number of waves of measurement, or measurement moments, required for reliable modeling, and compare explanatory models to select the most suitable option.

We will discuss the advantages of applying structural constancy tests, including various versions of these tests as used in linear regression and time series analysis, and explore how these tools can provide additional layers of insight beyond traditional model fit indices.

Structural Constancy Tests, in Linear Regression and in Time Series

Suppose you have a data set that follows a linear regression pattern. To evaluate whether the relationship between variables is consistent or changes significantly at a specific point, the Chow test (1960) can detect such change points. This test assesses whether splitting the data into two segments and fitting separate regressions improves model fit compared to using a single regression for the entire data set. The Chow test has a long history and is widely cited and explained in manuals, with various adaptations for specific cases. However, it has not been widely applied in the analysis of real-world data, perhaps because authors assume no structural break in the data, or they fear that journals may reject the article if such a structural break exists.

The procedure for conducting the Chow test in cross-sectional linear regression involves several steps (DeMaris, 2004; Gujarati et al., 2013): (a) Initiate linear regression analysis across the entire data set, employing a standard linear regression model to establish the best fitting line for all data points collectively (Figure 1A). This pooled regression yields a sum of squares of the pooled residuals (SSR_P). (b) Subdivide the data set into two distinct groups based on a predetermined criterion or hypothesis, labeled as groups A and B. For instance, in a cross-sectional study comparing educational

Figure 1
Lines Regression in a Chow Test

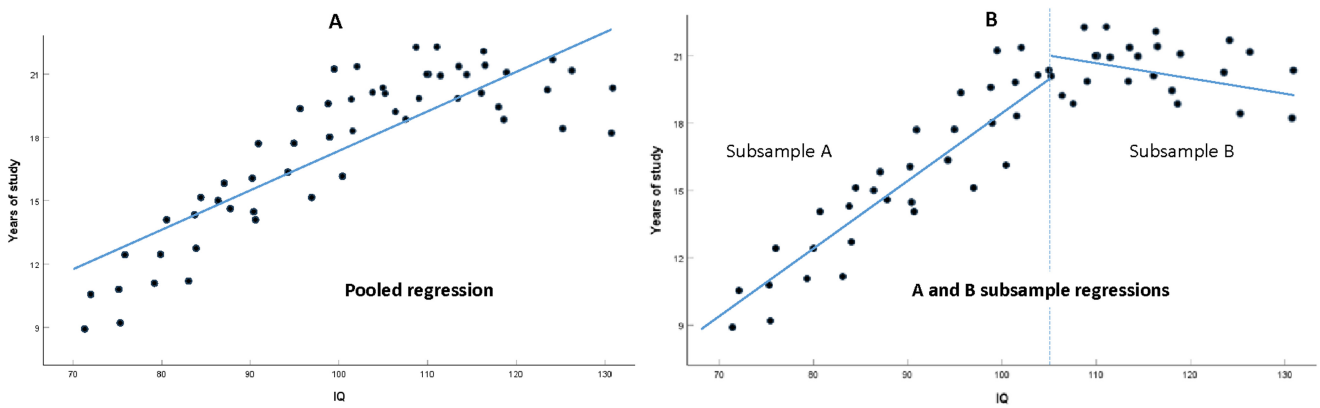

Note. (A) Shows lineal regression with the complete sample. (B) Shows a breakpoint between the two subsamples. IQ = intellectual quotient. See the online article for the color version of this figure.

achievement levels among students based on their intellectual quotient (IQ; Figure 1B). (c) Fit separate regression lines for each group of data points, resulting in respective sums of squares of the residuals for Groups A (SSR_A) and B (SSR_B). These lines may exhibit varying slopes or intercepts, suggesting potential changes in the relationship between variables across the two groups. (d) Calculate the Chow statistic by evaluating the disparity between the sum of squared errors for the separate regression lines and that of the combined line, $SSR_P - SSR_A - SSR_B$. This statistic gauges the adequacy of the lines in fitting the data. If SSR_P equals $SSR_A + SSR_B$, the pooled and the two groups' regression lines coincide. A breakpoint is indicated when $SSR_P > (SSR_A + SSR_B)$, meaning significantly larger residuals in the pooled regression compared to the two separated linear regressions. In Figure 1A and 1B, a simulated depiction of the relationship between years of study (Y axis) and IQ (X axis) is presented. Notably, there appears to be a breakpoint around an IQ value of approximately 105 on the X axis (a breakpoint exhibiting a lack of internal consistency relative to the initial pooled model). Consequently, the function depicted in Figure 1A and 1B lacks structural stability. Lee (2008) applied the Chow test across three different cases. In the first case, he examined the impact of placement in gifted educational programs on student achievement, with IQ as the independent variable (IV). The results showed no evidence that participation in the gifted program led to higher achievement compared to students not in such a program. Additional examples can be found in Anselin (1990), Hites (2019), and Muggeo (2003).

In linear time series analysis, an adaptation of the Chow test serves to identify structural breaks but is tailored explicitly for time series data (Cuthbertson et al., 1992; Hendry, 2011). Suppose we have a time series comprising T data points. When suspecting a change in the statistical model at a specific point, $T1$, the following steps are undertaken: (a) Segment the time series into two parts, one with a length of $T1$ and the other with $T2 = T - T1$. (b) Fit the model to segment $T1$ according to the assumed model. (c) Forecast the values of $T2$ ($Y_{T1+1}, Y_{T1+2}, \ldots, Y_T$) using the parameters derived from segment $T1$. (d) Compare the variances of $T2$ and $T1$; equality suggests structural constancy, whereas a greater variance in $T2$ than in $T1$ indicates a breakpoint at value $T1$. Some examples can be found in Bai and Perron (2003), Cooper et al. (2003) , Dao (2022), Hansen (2001), and Luitel and Mahar (2015).

LGC Models

To outline the basic formulation systems of LGC models, two distinct approaches have been prominent. The first employs polynomial linear functions (such as straight line, quadratic, and cubic), which have been widely adopted in research publications (e.g., Johnson & Hancock, 2019; Laursen et al., 2013; T. G. Little et al., 2007) and textbooks (Bollen & Curran, 2006; Ferrer et al., 2019; Grimm & Ram, 2018; T. G. Little, 2013; Preacher et al., 2008; Wood, 2011).

The second approach utilizes nonlinear functions (Blozis et al., 2008; Ferrer & McArdle, 2003; Grimm & Ram, 2009, 2018; Grimm et al., 2017; Harring et al., 2012; Laursen et al., 2013), which encompass several variations. These may involve the IV time appearing in the denominator of a fraction (as in Michaelis–Menten or Shinozaki–Kira), or the use of logarithmic or exponential functions (Blozis et al., 2008; Dziak et al., 2015; Harring et al., 2012; Konishi, 2014; Marcoulides, 2018; McNeish & Dumas, 2017; Panik, 2014; Preacher & Hancock, 2015; Ratkowsky, 1990; Seber & Wild, 2003).

The landscape of modeling options is diverse, yet ideally, the relationships between variables should be informed by a robust theoretical framework concerning the nature of the studied variables and hypotheses regarding the trajectory of developmental curves (Collins, 2006; Curran et al., 2010; Jaccard & Jacoby, 2020). However, despite the widespread use of the quadratic function (QF) model in this domain, it remains unclear why this model is favored over alternative approaches in the exploration of human development or learning.

The study of developmental curves using nonlinear models presents several challenges. Firstly, there exists a plethora of nonlinear models, none of which holds theoretical superiority over the others (Aslin, 1993; Cheung, 2014; W. Johnson, 2022; Molenaar & Newell, 1998; Panik, 2014). Secondly, some models exhibit minimal graphical differences in their representation. Thirdly, achieving parameter convergence across different statistical programs is often challenging (Bates & Watts, 2007; Cudeck & Harring, 2007; Gallant, 2009; Geiser, 2021; Grimm et al., 2017; Konishi, 2014; Ratkowsky, 1990; Seber & Wild, 2003; Willett & Sayer, 1994; Wood, 2011). Consequently, it has been suggested that the selection of a nonlinear model should consider not only its theoretical validity and statistical adequacy but also the interpretability of its parameters and the clarity of graphical data representation (Bates & Watts, 2007; Cudeck & Harring, 2007).

Nonlinear models are categorized into three main groups based on their graphical representation: those without an inflection point, those with one inflection point, and curves featuring a maximum point and two inflection points (e.g., Beta, Gauss, Gamma). In developmental and learning research fields such as psychology, education, and biology, only the first two types, with and without one inflection point, are recommended. Models lacking an inflection point are valuable for statistically modeling the final phase of growth or learning, revealing asymptotic maximum trend values and patterns of cognitive decline and memory loss, with the curve displaying an asymptotic minimum value. Various curves, including nonlinear, negative exponential (NEXP; Brody, 1945; Stevens, 1951), monomolecular growth curves (Seber & Wild, 2003), and the Michaelis and Menten function (2011), can be employed.

In the absence of a clear hypothesis guiding the selection of the most suitable explanatory model for the data, researchers often rely on goodness-of-fit indicators such as χ^2, AIC, Bayesian information criterion, and RMSEA (Bentler & Satorra, 2010; Satorra & Bentler, 2010; Bianconcini, 2012; Wu et al., 2009; Ye & Bollen, 2022). However, dynamic modeling theory establishes specific requirements for temporal statistical models applied to longitudinal data sets (Hendry, 1995; Pesaran, 2016). Essentially, the temporal behavior originates from a DGP that must adhere to a consistent statistical model. This means that the DGP cannot be explained using different equations or parameters across different segments of its trajectory, a property known as structural constancy. Structural stability is assessed through internal parameter stability or parameter constancy.

Conceptually, parameter stability in a model is akin to its statistical internal validity (Shadish et al., 2002). The PCT serves as a method to verify whether the statistical relationship established between the IV time and the dependent variable (DV) Y_t, with T measurements, remains intact even under more stringent temporal conditions (e.g., considering trimmed temporal values from right to left: $T - 1$, $T - 2$, etc.).

In developmental models, both the mean and the variance can change over time. For instance, in a learning or cognitive developmental process, the trajectory might exhibit a monotonically increasing curve ($Y_1 \leq Y_2 \leq \cdots \leq Y_t \leq \cdots \leq Y_{T-1} \leq Y_T$), with Y_T representing a limiting value and typically: $(Y_T - Y_{T-1}) \leq (Y_{T-1} - Y_{T-2})$. This indicates that the differences between consecutive values decrease as the process progresses, suggesting asymptotic growth toward the end of development. Additionally, the variance tends to slightly increase with time. The observation of varying growth rates along this trajectory implies a formal nonlinear relationship between time and Y_t.

Upon reviewing the NEXP models used in psychology, we found that while there are comparisons of models applied to specific data sets, there are no publications that comprehensively compare different linear and nonlinear models based on their statistical fit and the theoretical properties of an ideal growth model. Nonetheless, some research has identified the NEXP model as the best or among the best models for fitting real data (Chen et al., 2002; Kail & Ferrer, 2007; Murayama et al., 2013; Neale & McArdle, 2000).

PCT in LGCs

We have observed that tests for parameter constancy in linear regression and time series typically utilize sums of squares or variances for comparing temporal segments. However, in SEM, the assessment of fit differs from this approach. Instead of examining residuals' errors, the overarching hypothesis posits a set of parameters, denoted as θ_T, for the T moments. This hypothesis suggests that the covariance matrix with observed data, $\boldsymbol{S_T}$, should equal the estimated matrix derived from the model's involved values, denoted as $\boldsymbol{\Sigma(\theta_T)}$. The null hypothesis states: $\boldsymbol{S_T = \Sigma(\theta_T)}$.

To conduct a PCT in LGC, four steps are involved: (i) Initially, the fit with the entire data set, in our example with $T = 6$ [$\boldsymbol{S_T = \Sigma(\theta_T)}$], is computed, referred to as the complete free model. (ii) Subsequently, the last $T2$ temporal values for all individuals in the sample ($T1 + T2 = T$) are removed, and the model is estimated using only the first $T1$ temporal values, with all parameters freed. This yields new parameters, denoted as $\boldsymbol{\theta_{T1}}$, constituting what we term the unrestricted trimmed model. (iii) The entire T series is reanalyzed, imposing parameters from the $T1$ temporal values ($\boldsymbol{\theta_{T1}}$) on the model through corresponding constraints. This results in $\boldsymbol{S_{T(T1)}}$ (Chou & Bentler, 2002), designated as the T complete restricted model with $T1$ parameters. (iv) It is expected that if the unrestricted trimmed model of $T1$ waves of measurement is stable with respect to the complete model with the T moments, then $\boldsymbol{S_{T(T1)} = \Sigma(\theta_T)}$. That is, the complete model restricted with the parameters of $T1$, $\boldsymbol{S_{T(T1)}}$, must not differ from the complete free model, $\boldsymbol{\Sigma(\theta_T)}$. To verify this, since the model of the matrix for the restricted data, $\boldsymbol{S_{T(T1)}}$, is nested within the model corresponding to $\boldsymbol{\Sigma(\theta_T)}$, the contrast hypothesis test can be carried out using the χ^2 difference test of goodness-of-fit, with its corresponding degrees of freedom, to compare the equality of both matrices (Bentler & Satorra, 2010). If the complete model is correct, with $\boldsymbol{S_T = \Sigma(\theta_T)}$, then the restricted complete model with the parameters of $T1$ ($\boldsymbol{\theta_{T1}}$) will not differ from the complete free model, $\boldsymbol{S_{T(T1)} = \Sigma(\theta_T)}$. The basic idea is that there should be no structural change. These steps systematically test whether trimming temporal observations impacts the consistency of model parameters, thereby assessing the constancy of the entire model.

In our examples, we employ not only the χ^2 difference test but also various overall fit indicators (AIC, comparative fit index [CFI], Tucker–Lewis index [TLI], standardized root-mean-square residual [SRMR], and RMSEA) as comparison criteria. Concerning the PCT in LGC, a pertinent question arises: which parameters of the model with $T1$ temporal values need to be constrained in the model encompassing all values (i.e., with all waves T, Step (iii) of the PCT in LGC)? The answer lies in fixing the parameters governing the shape of the initial model (μ_α, $\mu_{\beta 1}$, $\mu_{\beta 2}$, …), as constraining the parameters of covariances ($\psi_{\alpha\beta_1}$, $\psi_{\alpha\beta_2}$, $\psi_{\beta_1\beta_2}$, …) and the variances of model parameters (ψ^2_α, $\psi^2_{\beta_1}$, $\psi^2_{\beta_2}$, …) would severely limit variability, hindering proper fitting. In our examples, attempts to restrict both shape and covariance parameters resulted in nonconvergence, prompting us to only restrict shape parameters. It should be noted that the greater the number of parameters is restricted, the less likely it is to achieve correct convergence of the final model $\boldsymbol{S_{T(T1)} = \Sigma(\theta_T)}$, or complete restricted model with $T1$ parameters.

In the Chow (1960) test, there is no specific recommendation regarding the number of values to consider for $T2$. Our suggestion is setting $T2 = 1$, then incrementing it sequentially ($T2 = 2$, $T2 = 3$, and so forth) until $\boldsymbol{S_{T(T1)} \neq \Sigma(\theta_T)}$. It is important to note that in our scenario, $T1$ should ideally be ≥ 3 to ensure an adequate number of time values for generating a curvilinear function, while also considering the model's degrees of freedom. Therefore, when comparing the constancy of different models, such as polynomial or nonlinear ones, the optimal model will be the one that demonstrates constancy with the fewest number of $T1$ moments using the PCT.

We can liken a temporal SEM model to a data set viewed through a window from a certain distance (Baird et al., 2021; Wagner et al., 2018). Essentially, we observe a series of T temporal data points from N individuals within this window, while recognizing that the series extends indefinitely into the future beyond the window's right edge, encompassing times $T + 1$, $T + 2$, and so forth. Although our observer cannot access these future data points from the current time sample, he can evaluate the model's stability based on its T waves of measurement. This process involves metaphorically closing the window to the future by concealing the view of the latest waves of measurement and sliding an imaginary curtain from right to left within the window. By doing so, the observer can assess the model's properties by progressively removing $T2$ observations.

Later, we will provide step-by-step examples showing how to conduct the respective PCT. Initially, we will outline the fundamental methodological characteristics of the QF, representing a polynomial LGC model, and elucidate the properties of the NEXP function as a nonlinear model. Subsequently, we will delve into PCT examples involving various other nonlinear models.

The Quadratic Growth Curve

The general formulation of an unconditional LGC, without exogenous IVs, is:

$$\mathbf{Y} = \boldsymbol{\Lambda\eta} + \boldsymbol{\varepsilon}, \tag{1}$$

where for one individual, $\mathbf{Y}$ is a $T \times 1$ vector of the measures (Y_{i1}, Y_{i2}, … , Y_{iT})′ of the observed DV, $\boldsymbol{\Lambda}$ is a $T \times m$ matrix of factor coefficients, being m the number of latent factors, $\boldsymbol{\eta}$ is a vector of $m \times 1$, representing the latent factors, and $\boldsymbol{\varepsilon}$ is a $T \times 1$ vector of residuals. When $\boldsymbol{\eta}$ is equal to a $m \times 1$vector of factor means $\boldsymbol{\mu_\eta}$, equal to (μ_α, $\mu_{\beta 1}$, $\mu_{\beta 2}$)′, plus a $m \times 1$vector of factor disturbances $\boldsymbol{\zeta}$, equal to

$(\zeta_{\alpha i}, \zeta_{\beta 1 i}, \zeta_{\beta 2 i})'$, then:

$$\mathbf{Y} = \mathbf{\Lambda}(\boldsymbol{\mu}_{\boldsymbol{\eta}} + \boldsymbol{\zeta}) + \boldsymbol{\varepsilon}. \tag{2}$$

In Equation 2, $\boldsymbol{\zeta}$ are the Level 2 deviations, or errors, including all the individuals of the sample with respect to the grand mean of each respective wave; and $\boldsymbol{\varepsilon}$ are the Level 1 errors, or the distance between the empirical data and the forecasted data for a particular individual of the sample.

For a model where a quadratic trajectory is postulated ($m = 3$), Equation 2 will be:

$$\begin{pmatrix} Y_{i1} \\ Y_{i2} \\ Y_{i3} \\ \vdots \\ Y_{iT} \end{pmatrix} = \begin{pmatrix} 1 & t_1 & t_1^2 \\ 1 & t_2 & t_2^2 \\ 1 & t_3 & t_3^2 \\ \vdots & \vdots & \vdots \\ 1 & T & T^2 \end{pmatrix} \begin{pmatrix} \propto_i \\ \beta_{1i} \\ \beta_{2i} \end{pmatrix} + \begin{pmatrix} \varepsilon_{i1} \\ \varepsilon_{i2} \\ \varepsilon_{i3} \\ \vdots \\ \varepsilon_{iT} \end{pmatrix}$$

$$= \begin{pmatrix} 1 & t_1 & t_1^2 \\ 1 & t_2 & t_2^2 \\ 1 & t_3 & t_3^2 \\ \vdots & \vdots & \vdots \\ 1 & T & T^2 \end{pmatrix} \begin{pmatrix} \mu_\alpha + \zeta_{\alpha i} \\ \mu_{\beta 1} + \zeta_{\beta 1 i} \\ \mu_{\beta 2} + \zeta_{\beta 2 i} \end{pmatrix} + \begin{pmatrix} \varepsilon_{i1} \\ \varepsilon_{i2} \\ \varepsilon_{i3} \\ \vdots \\ \varepsilon_{iT} \end{pmatrix}. \tag{3}$$

In any manual on LGC with SEM, we can find the properties of Equations 1 and 2, and of LGC in general. The $\mathbf{\Lambda}$ matrix is a set of fixed values for any SEM program, and the user has to provide these values.

If we obtain the algebraic QF in Equation 3, for any subject i and moment time:

$$Y_{it} = 1(\mu_\alpha + \zeta_{\alpha i}) + t_j(\mu_{\beta 1} + \zeta_{\beta 1 i}) + t_j^2(\mu_{\beta 2} + \zeta_{\beta 2 i}) + \varepsilon_{it}, \tag{4}$$

being Y_{it} the measured variable; 1, t_j, and ${t_j}^2$ are the respective time values (given by the user); μ_α is the intercept, or value of Y_i when time = 0, $\mu_{\beta 1}$ is the coefficient of the linear trend (t_j) of Equation 4, and $\mu_{\beta 2}$ is the common coefficient for the quadratic trend (${t_j}^2$); $\zeta_{\alpha i}$, $\zeta_{\beta 1 i}$, and $\zeta_{\beta 2 i}$ are the respective Level 2 factorial punctuations for the individual i in μ_α, $\mu_{\beta 1}$, and $\mu_{\beta 2}$, and can be thought as the deviations of the corresponding coefficients, as in any factor analysis; and ε_{it} is the Level 1 forecast error. So, the general mean forecasted values for all the subjects at moment time, Y_t', in Equation 4 will be:

$$Y_t' = \mu_\alpha + t_j\mu_{\beta 1} + t_j^2\mu_{\beta 2}. \tag{5}$$

Note that Equation 5 is a classic QF but employing different symbols.

The Cov($\boldsymbol{\eta}$) in Equations 2–4:

$$\mathrm{Cov}(\boldsymbol{\eta}) = \mathbf{\Psi} = \begin{pmatrix} \psi_\alpha^2 & \psi_{\alpha\beta 1} & \psi_{\alpha\beta 2} \\ \psi_{\alpha\beta 1} & \psi_{\beta 1}^2 & \psi_{\beta 1\beta 2} \\ \psi_{\alpha\beta 2} & \psi_{\beta 1\beta 2} & \psi_{\beta 2}^2 \end{pmatrix}. \tag{6}$$

In considering the above, we will study, in the context of SEM, the fit capability through a learning curve of an NEXP function in comparison with a QF.

The NEXP Function

The NEXP function has been used previously (Brody, 1945; Stevens, 1951):

$$Y_{it} = b_{0i} + b_{1i}(1 - e^{-b_{2}t}) + \varepsilon_{it}. \tag{7}$$

Equation 7 in the SEM modelization will be:

$$Y_{it} = 1(\mu_\alpha + \zeta_{\alpha i}) + (1 - e^{-b_{2}t})(\mu_{\beta 1} + \zeta_{\beta 1 i}) + \varepsilon_{it}. \tag{8}$$

Figure 2
Quadratic and NEXP Models

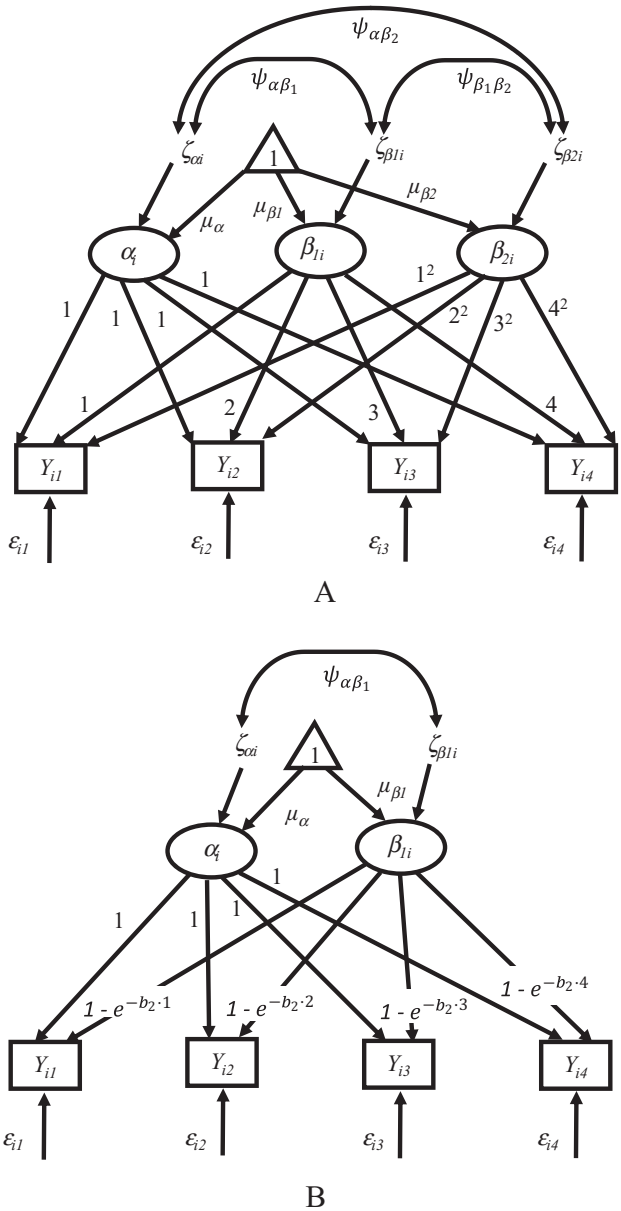

Note. Representation of a latent growth model, with two factors and $T = 4$ moments of measurement: (A) quadratic (polynomial) and (B) negative exponential, both with initial t coefficients: 1, 2, 3, and 4. NEXP = negative exponential.

Table 1
Descriptive Statistics and Pearson's Correlations of the Six Waves of Measurement for the ASV

ASV	*M*	*SD*	*N*	1	2	3	4	5	6
1. ASV1	11.631	7.297	141	—					
2. ASV2	21.156	8.723	141	.771***	—				
3. ASV3	27.305	8.939	141	.603***	.813***	—			
4. ASV4	30.879	9.271	140	.502***	.727***	.892***	—		
5. ASV5	32.393	9.079	140	.481***	.691***	.836***	.910***	—	
6. ASV6	34.204	9.844	137	.462***	.675***	.799***	.882***	.928***	—

Note. ASV = Armed Services Vocational Aptitude Battery variable.
*** $p < .001$.

The between-subjects Level 2 random variability of the parameters in Equation 7 (b_{0i} and b_{1i}) is transferred in Equation 8 to the variability of the factors ($\zeta_{\alpha i}$ and $\zeta_{\beta 1 i}$). Note that Equations 4 and 8 are very similar, except that in the quadratic Equation 4 the λ coefficients of the $\mathbf{\Lambda}$ matrix are t_j and ${t_j}^2$, while $(1 - e^{-b_2 t})$ is the NEXP coefficient of Equations 7 and 8.

If in Equation 3 we use $\mathbf{\Lambda}$ values corresponding to a QF, in an NEXP function, the $\mathbf{\Lambda}$ matrix will be:

$$\mathbf{\Lambda} = \begin{pmatrix} 1 & 1 - e^{-b_2 t_1} \\ 1 & 1 - e^{-b_2 t_2} \\ 1 & 1 - e^{-b_2 t_3} \\ \vdots & \vdots \\ 1 & 1 - e^{-b_2 t_T} \end{pmatrix}. \tag{9}$$

A caveat, once more, is that the values of the parameters ($\mu_j's$, $\zeta_j's$, $\psi_j^{2\prime}s$, $\psi_{j,k}'s$, ε_j's, Var(ε_j)'s …) are relative to each of the two models in Equations 4 and 8, and they will be different, that is, QF or NEXP, and we could obtain different values as a function of the model analysed. We could have used different symbols for each model (e.g., μ_j^Q for the quadratic and μ_j^{EXP} for the NEXP model), but we have chosen not to complicate the information included in the equations. To consider the previous notions and explain the PCT in a practical way, we will take a real data set (Kanfer & Ackerman, 1989, K&A from now on) and compare their corresponding statistical fits and properties using two models: a QF and an NEXP.

In Figure 2, there is a representation of each latent growth model in SEM: we show a QF in Figure 2A (that has three factors), and in Figure 2B the NEXP model, with its two factors and both with $T = 4$ moments of measurement. To represent the constants, we follow the system put forward by McArdle and Epstein (1987) in which the constants are distinguished by an arrow with a triangle placed at the origin with a number "1" inside it. The difference between the two models lies in the fixed effects from factors on the observed variables, but in Figure 2A, for the QF, α_i is the factor of 1 values, or constant, β_{1i} is the factor slope, and β_{2i} is the factor of quadratic values; in Figure 2B, α_i is the factor of 1 values, or constant, and β_{1i} is the factor of the NEXP model; and also this latest model has an

Figure 3
GM Profile, Thick Dashed Line, and Participants 1 (P1), 2 (P2), 3 (P3), 4 (P4), and 6 (P6)

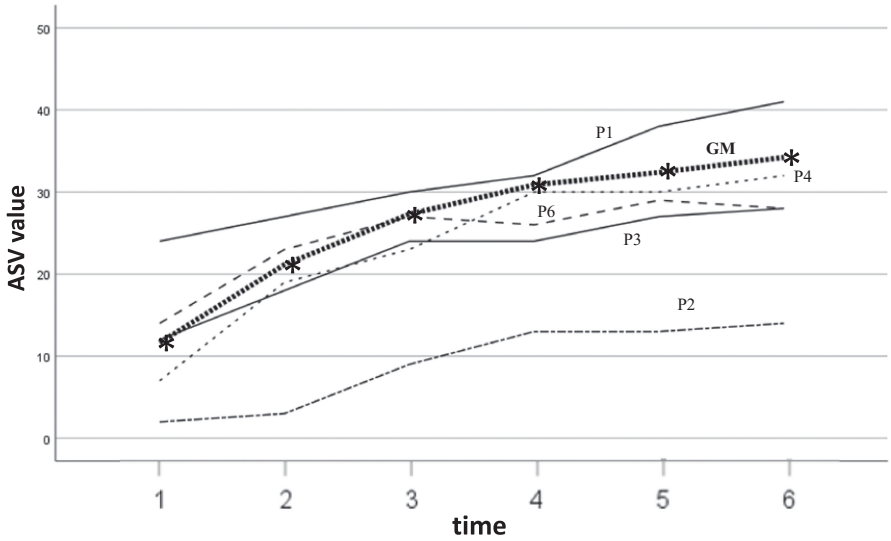

Note. We have not included P5 because its profile is almost equal to that of the great mean, being their profiles entangled. Asterisk indicates the GM of each moment of measurement; the other values of the line are interpolations. GM = grand mean; ASV = Armed Services Vocational Aptitude Battery variable.

internal coefficient in the second factor, β_{1i}, corresponding to the b_2 coefficient.

Hypothesis

We hypothesize that PCT is sufficiently sensitive to identify differences in parameter constancy across various models. This study employs PCT to compare the widely used QF model with nonlinear exponential models such as NEXP, Michaelis–Menten, Allometric, and Shinozaki–Kira. These models were chosen for their capability to capture monotonic growth processes relevant to developmental research. The QF model is widely used in manuals and applied research, while the nonlinear exponential models were selected for their comprehensive documentation in technical manuals and the presence of only one parameter in their equations. The choice of these nonlinear models is intentional: like the NEXP model, they include only one additional parameter and exhibit monotonic increases without an inflection point, mirroring typical learning curve processes. Consequently, we excluded other models used in child development or learning research, such as Jenss and Bayley (1937), SITAR (Cole et al., 2010) , and Berkey and Reed (1987), that do not share these characteristics. Likewise, attempts to fit the data to other nonlinear models with an inflection point, like the logistic and Gompertz models (adding only one parameter), did not achieve parameter convergence with the data set. We illustrate the application of the PCT using a longitudinal panel data set derived from a learning process.

Method

Data

We will conduct secondary data analysis of one set of data previously published in open access referred to learning in adults, using the Armed Services Vocational Aptitude Battery (ASV) variable (Browne & Du Toit, 1991; Kanfer & Ackerman, 1989), which were found in the files of LISREL8 (Jöreskog & Sörbom, 1996). It is a sample of 141 individuals in the U.S. Air Force who completed six trials of a computerized air traffic controller task, and there is not specification about age, gender, or any other personal characteristic; more details are available in the referenced Browne and Du Toit's (1991) article.

SPSS (2020), Mplus (Muthén & Muthén, 2021) and lavaan (Rosseel, 2012) data and input files are freely available at https://repositori.uji.es/items/f037c221-a043-4d1c-9385-f5c056b0bbad.

Statistical Analysis and Results

We will carry out the data analysis by first describing the descriptive results obtained with the original data, and then using the Quadratic Model and the Negative Exponential Model.

Descriptive Results

Means, standard deviations, and Pearson's correlations (r) of the six measurements of the ASV variable in the sample are shown in Table 1.

Table 2

Kanfer and Ackerman's Data ($T = 6$) Main Results in Latent Growth Curve SEM Analysis, Comparing the Quadratic and the Negative Exponential Model

Parameter	Quadratic model, value (*SE*)	NEXP model, value (*SE*)
μ_α	1.123 (0.842)	−5.190 (1.414)***
$\mu_{\beta 1}$	11.525 (0.520)***	40.478 (1.495)***
$\mu_{\beta 2}$	−1.017 (0.067)***	
ψ^2_α	97.440 (14.677)***	127.670 (20.168)***
$\psi^2_{\beta_1}$	30.251 (4.105)***	253.114 (27.553)***
$\psi^2_{\beta_2}$	0.391 (0.071)***	
$\psi_{\alpha\beta_1}$	−38.288 (5.511)***	−142.589 (20.977)***
$\psi_{\alpha\beta_2}$	3.991 (0.627)***	
$\psi_{\beta_1\beta_2}$	−3.310 (0.518)***	
b_2		0.537 (0.035)***
	Overall fit	
χ^2 (RML)[a]	61.001 (13)***	60.613 (16)***
Correction factor	1.158	1.121
AIC	5,099.703	5,090.936
CFI	.942	.946
TLI	.933	.949
SRMR	.052	.050
RMSEA	.162	.141
90% CI	[0.122, 0.204]	[0.104, 0.179]
p(RMSEA[a] $\leq$ .05)	***	***
	Long-run trend	
Y_∞	$-\infty$	35.558
Level 2 SE_B (Y_∞)	∞	9.778
95% CI (Y_∞)	[$-\infty$, $+\infty$]	[16.393, 54.723]

Note. SEM = structural equation modeling; NEXP = negative exponential; RML = robust maximum likelihood (Yuan & Bentler, 2000); AIC = Akaike information criterion; CFI = comparative fit index; TLI = Tucker–Lewis index; SRMR = standardized root-mean-square residual; RMSEA = root-mean-square error of approximation; CI = confidence interval.

[a] Probability of RMSEA.

*** $p < .001$.

In Figure 3, we have displayed the general mean of all the data as a function of the moment of measurement, and only five individuals of the sample, because if we add more individuals, the figure could be confusing.

As can be seen in Table 1 and Figure 3, the means follow a gradually increasing process, as expected of a classic learning curve, and the correlations between the repeated measured variables are all statistically significant. Table 1 shows a repeated measures structure, with high but decreasing correlations as the temporal distance between moments increases. The intraclass correlation (ICC) is .735, and its $F = 17.604(136, 680)$, $p < .001$; this high ICC indicates that the participants have profiles that are similar to one another. If we observe Figure 3, the participants have very similar profiles, and are similar to the average profile, differing from each other in the level of every profile, and with deviations being almost equidistant to the mean path of the participants.

Data Analysis: Quadratic "Versus" NEXP Models

In ASV1 to ASV3, the sample included 141 people. ASV4 and ASV5 were answered by 140, and ASV6 had 137 responses, so we have used missing data maximum likelihood estimation (R. G. Little & Rubin, 2019), with free values of the initial parameters. We have applied the Kolmogorov–Smirnov normality test, with the Lilliefors correction to the six variables, with ASV3, ASV4, and ASV5 being nonnormal; we have applied the Mardia's test (1970) for multivariate normality with missing values (Yuan et al., 2004), resulting in a value of 11.147, defining not multivariate normality, and so we have used the robust maximum likelihood estimator (Yuan & Bentler, 2000). Due to the nonnormality of data, the scarce number of subjects in the sample and the very few degrees of freedom, for comparison of χ^2 in nested models, we will do the Asparouhov and Muthén (2006, 2010) scaled χ^2 difference between models, $\Delta\chi^2(\Delta df)$, considering the difference in χ^2 values and their respective variances (Pavlov et al., 2020).

Quadratic Model

According to the results obtained for the QF in Table 2 and substituting values in Equation 5, the forecasted values of the final equation are:

$$Y'_t = \mu_\alpha + t_j\mu_{\beta 1} + t_j^2\mu_{\beta 2} = 1.123 + t_j \cdot 11.525 + t_j^2(-1.017). \quad (10)$$

With the aim of simplifying the calculus, in Table 3 we develop several types of polynomials (degree 1, 2, and 3) and some of the most used nonlinear models without inflection point, with only an additional parameter, b_2 (Michaelis–Menten, monomolecular, allometric and Shinozaki–Kira), with a quick demonstration of their LRT values (Y_∞) when time trends to infinitive value (Panik, 2014), and the Level 2 variance of the forecasted general mean values, $\mathrm{Var}_B(Y')$.

On Figure 4A there is a representation of the expected general mean values of the QF, formulated in Equation 10, and its 95% confidence interval (CI) of Level 2 general mean; Equation 10 (Figure 4A) has a maximum value on Y' when the moment of measurement is time = 5.50, yielding a value of $Y'_{t=5.50} = 33.746$, which is no coherent with the data, and the expected QF mean for time = 6 is 33.661, but the real maximum value is obtained when time = 6

Table 3
Forecasted Values (Y'), Long-Run Trend (Y_∞), and Their Level 2 Variances, Var_B (Y_∞), on Long-Run Trend, in Polynomial and Nonlinear Models

Model	Arithmetic equation	SEM equation	$Y_\infty(t \to \infty)$	Level 2 Var_B (Y_∞)
Polynomial models				
Degree 1, straight line	$Y' = b_0 + b_1 t$	$Y' = \mu_\alpha + \mu_{\beta 1} t$	$Y_\infty = \pm\infty$[a]	$\mathrm{Var}(Y_\infty) = \psi^2_\alpha + t^2\psi^2_{\beta_1} + 2\psi_{\alpha\beta_1} = \infty$[a]
Degree 2, quadratic line	$Y' = b_0 + b_1 t + b_2 t^2$	$Y' = \mu_\alpha + \mu_{\beta 1} t + \mu_{\beta 2} t^2$	$Y_\infty = \pm\infty$[a]	$\mathrm{Var}(Y_\infty) = \psi^2_\alpha + \psi^2_{\beta_1} t^2 + \psi^2_{\beta_2} t^4 + 2\psi_{\alpha\beta_1} t + 2\psi_{\alpha\beta_2} t^2 + 2\psi_{\beta_1\beta_2} t^3 = \infty$[a]
Degree 3, cubic line	$Y' = b_0 + b_1 t + b_2 t^2 + b_3 t^3$	$Y' = \mu_\alpha + \mu_{\beta 1} t + \mu_{\beta 2} t^2 + \mu_{\beta 3} t^3$	$Y_\infty = \pm\infty$[a]	$\mathrm{Var}(Y_\infty) = \psi^2_\alpha + \psi^2_{\beta_1} t^2 + \psi^2_{\beta_2} t^4 + \psi^2_{\beta_3} t^6 + 2\psi_{\alpha\beta_1} t + 2\psi_{\alpha\beta_2} t^2 + 2\psi_{\alpha\beta_3} t^3 + 2\psi_{\beta_1\beta_2} t^3 + 2\psi_{\beta_1\beta_3} t^4 + 2\psi_{\beta_2\beta_3} t^5 = \infty$[a]
Nonlinear models				
Negative exponential	$Y' = b_0 + b_1(1 - e^{-b_2 t})$	$Y' = \mu_\alpha + \mu_{\beta 1}(1 - e^{-b_2 t})$	$Y_\infty = \mu + \mu_{\beta 1}$	$\mathrm{Var}(Y_\infty) = \psi^2_\alpha + \psi^2_{\beta_1} + 2\psi_{\alpha\beta_1}$
Michaelis–Menten	$Y' = b_0 + b_1(t/(b_2 + t)$	$Y' = \mu_\alpha + \mu_{\beta 1}(t/(b_2 + t)$	$Y_\infty = \mu_\alpha + \mu_{\beta 1}$	$\mathrm{Var}(Y_\infty) = \psi^2_\alpha + \psi^2_{\beta_1} + 2\psi_{\alpha\beta_1}$
Monomolecular	$Y' = b_0 + b_1 e^{-b_2 t}$	$Y' = \mu_\alpha + \mu_{\beta 1} e^{-b_2 t}$	$Y_\infty = \mu_\alpha + \mu_{\beta 1} 0 = \mu_\alpha$	$\mathrm{Var}(Y_\infty) = \psi^2_\alpha + \psi^2_{\beta_1} 0 + 2\psi_{\alpha\beta_1} 0 = \psi^2_\alpha$
Allometric[b]	(a) $Y' = b_0 + b_1 t^{b_2}$ (b) $Y' = b_0 + b_1 t^{-b_2}$	$Y' = \mu_\alpha + \mu_{\beta 1} t^{b_2}$ $Y' = \mu_\alpha + \mu_{\beta 1} t^{-b_2}$	$Y_\infty = \infty$[a] $Y_\infty = \mu_\alpha + 0 = \mu_\alpha$	$\mathrm{Var}(Y_\infty) = \psi^2_\alpha + \infty\psi^2_{\beta_1} + 2\infty\psi_{\alpha\beta_1} = \infty$[a] $\mathrm{Var}(Y_\infty) = \psi^2_\alpha + 0\psi^2_{\beta_1} + 20\psi_{\alpha\beta_1} = \psi^2_\alpha$
Shinozaki–Kira	$Y' = b_0 + b_1(1/(b_2 + t))$	$Y' = \mu_\alpha + \mu_{\beta 1}(1/(b_2 + t))$	$Y_\infty = \mu_\alpha + 0\mu_{\beta 1} = \mu_\alpha$	$\mathrm{Var}(Y_\infty) = \psi^2_\alpha$

Note. SEM = structural equation modeling.
[a] The positive allometric, option (a), and all the polynomial models are not bounded, so they must be avoided. [b] The bounded condition in an allometric model: $b_2 < 0$, which means that the value of the parameter must be negative; we develop the two versions of the allometric model, but only negative option (b) is bounded.

Figure 4

Forecasted Values and Their 95% Confidence Intervals From a Quadratic Model, Showing Predictions for T = 6 Based on Either All Available Data (A), Data Up to T1 = 5 (B), or Data Up to T1 = 4 (C)

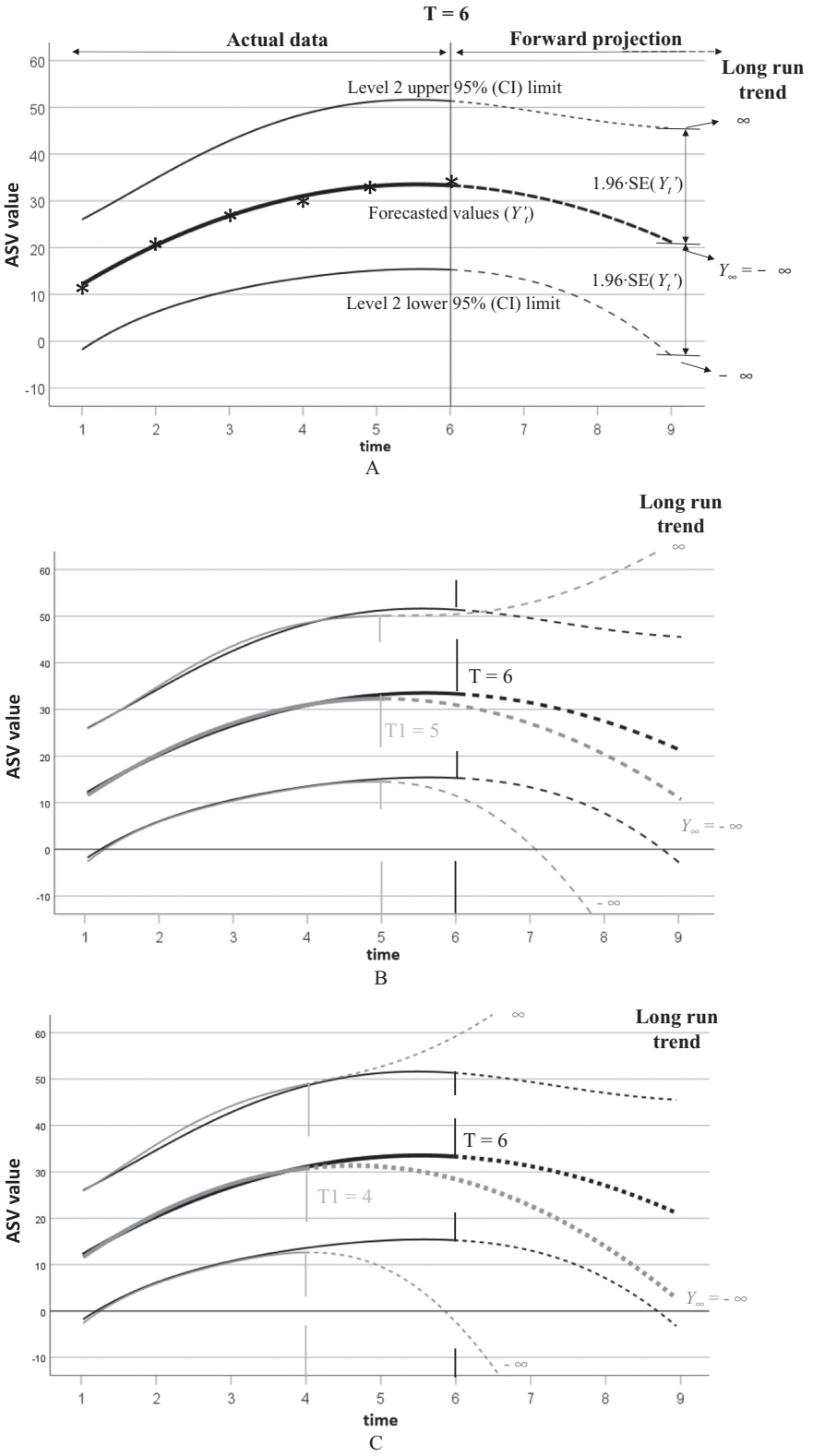

(*figure continues*)

($\bar{Y}_{\text{time}=6} = 34.204$), so the real values trend is ascendant and the QF is not, descending from time = 5.50.

NEXP Model

If we consider Equation 7 and Table 2, substituting the results, we can obtain the forecasted values:

$$Y'_t = \mu_\alpha + (1 - e^{-b_2 t})\mu_{\beta 1} = -5.190 + (1 - e^{-.537t})40.478. \quad (11)$$

Equation 11 is more consistent with the data than Equation 10, as it is monotonically increasing, as seen in Figure 5, having a maximum value of Y' in time = 6, $Y'_t = 33.783$.

Models Fit Comparison

When examining the fit of each model separately, it turns out that the quadratic fit is correct for the data. We see in Table 2 that CFI, TLI, and standardized root-mean-square residual statistics show a good fit, but the χ^2/df ratio and RMSEA are not good, so we can accept the QF as an adequate model describing the original data. On the other hand, the overall fit indicators of the NEXP model are better, the χ^2/df ratio is better too, but bigger than 2, and both the CFI and the TLI present a good fit (>.95) such that this model presents a slightly better good overall fit to the data.

The AIC values are for the QF 5,099.703, and for the NEXP model 5,090.936, so the empirical increment is $\Delta_{i(\text{AIC})} = 8.767$, bigger than 7 (Burnham & Anderson, 2004; Burnham et al., 2011; Claeskens & Hjort, 2010); in brief, the difference shows that, in this case and across the entire data set, the fit of the NEXP model is more sustainable than the quadratic.

PCT Analisys

In the paragraph about "parameter constancy test" we have described the four steps recommended for running the PCT; so, we will start by examining the PCT of the QF, to then proceed on to the NEXP model, and we will finally compare the results of both models.

Quadratic Model

If we revisit the four steps for running the PCT in the paragraph about "parameter constancy test" applied to the QF, we have:

(i) Shown that complete free model, $\boldsymbol{S_T}$, of the QF with all the data ($T = 6$) is, according to global fit indicators, an acceptable representation of the data (Table 2).

(ii) Cut the series, making unrestricted trimmed model parameters, deleting the measurements of the sixth wave ($T2 = 1$) of all the participants in the research, first, and deleting the last two waves ($T2 = 2$) of measurement of the data, after. We do not represent the results of $T2 = 3$, because the *df* have a negative value, and the model cannot be estimated. The results of $T1 = 5$ and $T1 = 4$ appear in Table 4, and we can see that the overall fit of both models is good. However, we are not interested in these results but in the values of the parameters μ_α, $\mu_{\beta 1}$, and $\mu_{\beta 2}$, with the aim of using them as fixed parameters in the respective models $\boldsymbol{S_{T(T1)}}$.

Trimming the values for the last moment of measurement ($T2 = 1$), leaving the model $T1 = 5$, according to the results obtained for the QF in Table 4, and substituting values in Equation 5, the general mean forecasted values of the final equation for $T1 = 5$, are:

$$Y'_t = -0.135 + t_j \times 13.087 + t_j^2(-1.320). \quad (12)$$

In Figure 4B we show the representation of QF with $T1 = 5$, corresponding to temporal forecasts according to Equation 12, and its level two 95% CI.

Taking the results obtained for the QF in Table 4 for $T1 = 4$, and substituting values in Equation 5, the forecasted values of the final equation are:

$$Y'_t = -0.742 + t_j \times 13.871 + t_j^2(-1.498). \quad (13)$$

In Figure 4C, we show the representation of QF with $T1 = 4$, for the forecast of the observed values, and for the level two 95% CI of the predicted mean values, according to Equation 13. In Figure 4B and 4C, we have indicated the forecasted values for $T = 6$, with a grey color, in order to be able to directly compare the results of the different curves with the original curve $T = 6$. It can be observed that from $T1 = 5$ or from $T1 = 4$, the forecast of the values for all the data of $T = 6$ is not good, both in their expected values for $T = 6$, and in the CI of the forecasts.

(iii) If we take the results obtained in Table 4, of complete T restricted model with the parameters of $T1$, and copy the values of the shape parameters of the QF μ_α, $\mu_{\beta 1}$, and $\mu_{\beta 2}$, from the analyses of the trimmed samples $T1 = 5$ and $T1 = 4$, generating the respective complete restricted models with the parameters of $T1$, so that now those values of the parameters, μ_α, $\mu_{\beta 1}$, and $\mu_{\beta 2}$, are set as input values in the sample for all data, $\boldsymbol{S_{6(T1=5)}}$ and $\boldsymbol{S_{6(T1=4)}}$, then we generate the overall fit results shown in Table 5.

(iv) The contrast hypothesis test results of $\boldsymbol{S_T = \Sigma(\theta_T)}$ are shown at the bottom of Table 5. In the statistical contrast between the original results ($T = 6$) with the model of all data, but imposing the shape parameters of $T1 = 5$ using all data, the difference, $\Delta\chi^2(\Delta df)$, gives the result 40.793(3),with $p < .001$ [$\boldsymbol{S_{6(T1=5)}} \neq$

Figure 4 (*continued*)

Note. Forecasted values, with Level 2 upper and lower at 95% CI limits, according to the quadratic model: (A) with all values, $T = 6$, and their projection; (B) with $T1 = 5$ and the projection (gray Line), and $T = 6$ (Black Color); and (C) with the projection of $T1 = 4$ (gray line) and $T = 6$ (black color). Asterisk indicates the grand mean of each moment of measurement on Panel (A). On Panels (B) and (C), we have left the forecasted values for $T = 6$, with a black color always, in order to be able to directly compare the results of the different curves. ASV = Armed Services Vocational Aptitude Battery variable; CI = confidence interval; $T1$ = our or five measurement moments.

Figure 5

Forecasted Values and Their 95% Confidence Intervals From a NEXP Model, Showing Predictions for T = 6 Based on Either All Available Data (A), Data Up to T1 = 5 (B), or Data Up to T1 = 4 (C)

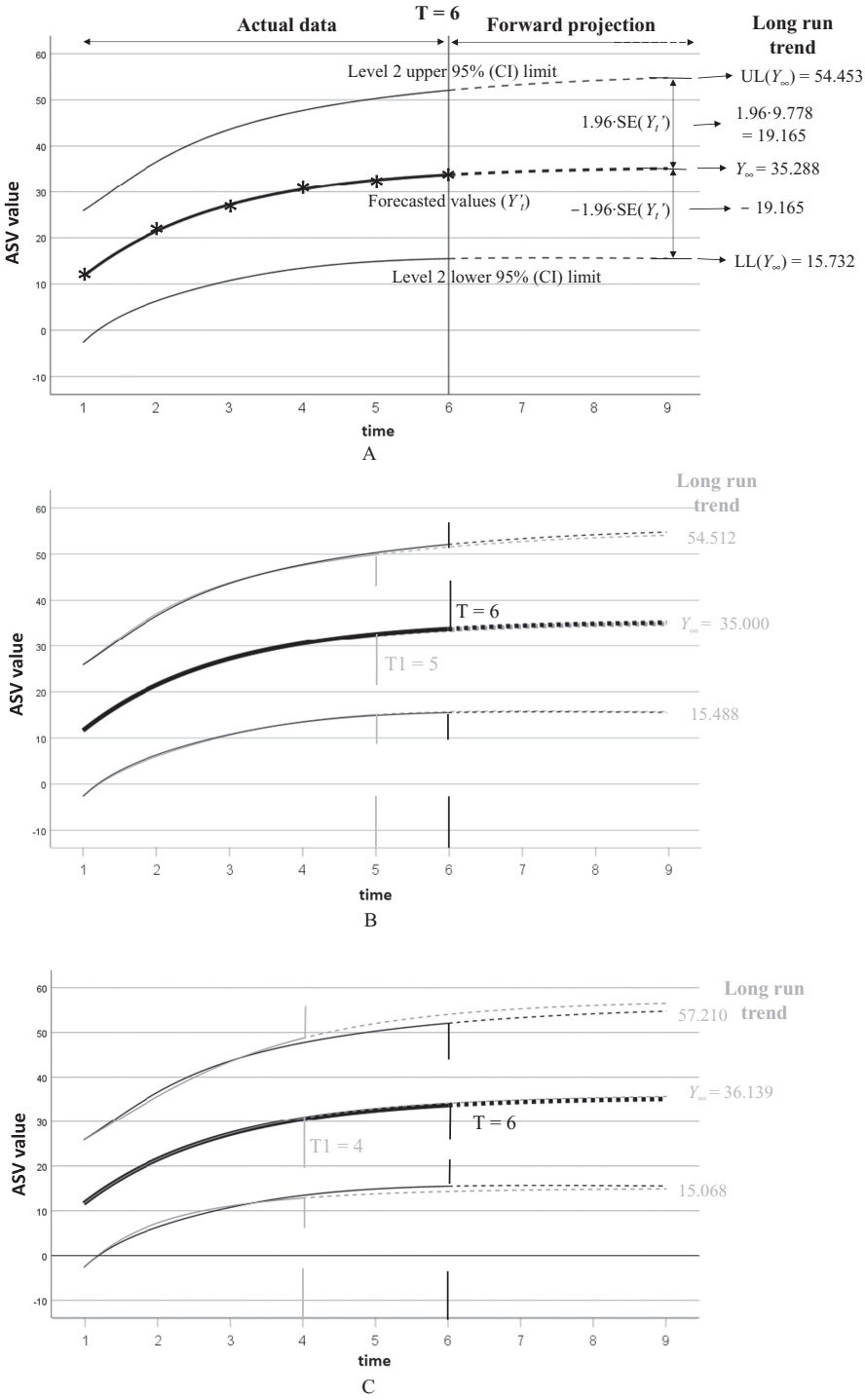

Note. Forecasted values, with Level 2 upper and lower at 95% CI limits, according to the negative exponential model: (A) with all data $T = 6$; (B) with $T1 = 5$ and its projection (gray line) and $T = 6$ (black color); and (C) with the projection of $T1 = 4$ (gray line) and $T = 6$ (black color). Asterisk indicates the grand mean of each moment of measurement on Panel (A). On Panels (B) and (C) we have left the forecasted values for $T = 6$, with a black color, in order to be able to directly compare the results of the different curves. ASV = Armed Services Vocational Aptitude Battery variable; CI = confidence interval; *UL* = upper limit; *LL* = lower limit; *T*1 = four or five measurement moments; NEXP = negative exponential.

Table 4
Parameter Stability Tests' Main Results for the Quadratic Model, in Function of the Trimmed Last Values

Trimming Parameter	$T1 = 5$ ($T2 = 1$) Value (*SE*)	$T1 = 4$ ($T2 = 2$) Value (*SE*)
	Quadratic model	
μ_α	−0.135 (0.885)[a]	−0.742 (0.959)[b]
$\mu_{\beta 1}$	13.087 (0.624)***[a]	13.871 (0.801)***[b]
$\mu_{\beta 2}$	−1.320 (0.090)***[a]	−1.498 (0.144)***[b]
ψ^2_α	106.511 (15.203)***[a]	108.091 (17.482)***[b]
$\psi^2_{\beta_1}$	47.859 (6.828)***	58.916 (11.900)***
$\psi^2_{\beta_2}$	0.924 (0.181)***	1.621 (0.597)**
$\psi_{\alpha\beta_1}$	−51.019 (7.651)***	−56.340 (11.768)***
$\psi_{\alpha\beta_2}$	6.199 (1.125)***	7.632 (2.237)**
$\psi_{\beta_1\beta_2}$	−6.391 (1.072)***	−9.170 (2.507)***
	Overall fit	
χ^2 (RML)	8.543 (7), $p = .287$	1.812 (2), $p = .404$
Correction factor	1.017	1.083
AIC	4,302.034	3,527.988
CFI	.998	1.000
TLI	.996	1.001
SRMR	.019	.022
RMSEA	.040	.000
90% CI	[0.000, 0.116]	[0.000, 0.162]
p(RMSEA)[c] $\leq .05$	.510	.521
	Long-run trend	
Y_∞	$-\infty$	$-\infty$
Level 2 *SE* (Y_∞)	∞	∞
95% CI (Y_∞)	$[-\infty,+\infty]$	$[-\infty,+\infty]$

Note. Values with superscript letters indicate the freely estimated values in Table 4 that will be used as the initial fixed values to fit the quadratic models in Table 5. $T1$ = number of waves used; $T2$ = number of waves deleted, being: $T1 + T2 = 6$. RML = robust maximum likelihood; AIC = Akaike information criterion; CFI = comparative fit index; TLI = Tucker–Lewis index; SRMR = standardized root-mean-square residual; RMSEA = root-mean-square error of approximation; CI = confidence interval.
[a] Initial fixed value for model $\boldsymbol{S_{6(T1=5)}}$. [b] Initial fixed value for model $\boldsymbol{S_{6(T1=4)}}$. [c] Probability of RMSEA.
** $p < .01$. *** $p < .001$.

$\boldsymbol{\Sigma(\theta_6)}$], and the original QF with $T1 = 5$ in Table 2 is not stable in their parameters at the PCT in comparison with all data fit ($T = 6$). We have also made the statistical comparison between the $T = 6$ data and the $T1 = 4$, constraining over $T = 6$ the shape parameters of $T1 = 4$. As a result, $\Delta\chi^2(\Delta df)$ is 92.147(3), $p < .001$, so as expected (because for $T1 = 5$ the data do not fit), we reject the equality of both models $[\boldsymbol{S_{6(T1=4)}} \neq \boldsymbol{\Sigma(\theta_6)}]$.

After applying the PCT, the QF is not internally stable in its shape, neither for $T1 = 5$ nor for $T1 = 4$, when it is applied to the $T = 6$ of the entire sample.

NEXP Model

We next reviewed the four-step procedure to run the PCT explained in the section on "parameter constancy test":

(i) We have seen in Table 2 that the NEXP model is an acceptable representation of our data; this is now our complete free model, so we will evaluate its internal structural stability, comparing $T1 = 5$, $T1 = 4$, and $T1 = 3$ with the complete data $T = 6$.

(ii) Trimming the values for the last moment of measurement, $T2 = 1$, leaving the model $T1 = 5$, and using the results on Table 6, if we take Equation 7, and substitute the results obtained in Table 6 for $T1 = 5$, then we can obtain the forecasted values on the NEXP model:

$$Y'_t = -5.738 + (1 - e^{-.556t})40.738. \quad (14)$$

In Figure 5B, we show a representation of the general mean and its 95% CI of the NEXP model with $T1 = 5$, in agreement with Equation 14.

Similarly, considering the results for $T1 = 4$ from Table 6, and taking them to Equation 7 for the forecast total mean of values:

$$Y'_t = -4.528 + (1 - e^{-.506t})40.667. \quad (15)$$

It is straightforward to obtain the forecasting equation based on the result values in Table 6 for $T1 = 3$: $Y'_t = -2.782 + (1 - e^{-.420t})42.008$.

In Figure 5C, we show a representation of NEXP model with $T1 = 4$, for the forecast of the observed values, according to Equation 15. In both Figure 5B and 5C, we have left the forecasted values for $T = 6$, from Equation 15, in grey color, while the predicted values from Equation 7 are in black, so that we can directly compare

Table 5
Results of the PTS for the Quadratic Model

Parameter	$S_{6(T1=5)}$ Value (*SE*)	$S_{6(T1=4)}$ Value (*SE*)
	Quadratic model	
μ_α	−0.135[a]	−0.742[b]
$\mu_{\beta 1}$	13.087[a]	13.871[b]
$\mu_{\beta 2}$	−1.320[a]	−1.498[b]
ψ^2_α	97.890 (15.041)***	99.941 (15.518)***
$\psi^2_{\beta_1}$	32.354 (4.496)***	35.371 (4.997)***
$\psi^2_{\beta_2}$	0.444 (0.087)***	0.560 (0.106)***
$\psi_{\alpha\beta_1}$	−39.374 (5.762)***	−41.908 (6.125)***
$\psi_{\alpha\beta_2}$	4.157 (0.695)***	4.656 (0.795)***
$\psi_{\beta_1\beta_2}$	−3.655 (0.605)***	−4.248 (0.708)***
	Overall fit	
χ^2 (RML)	98.980 (16)***	144.419 (16)***
Correction factor	1.125	1.128
AIC	5,134.329	5,185.850
CFI	.900	.845
TLI	.906	.854
SRMR	.083	.022
RMSEA	.192	.239
90% CI	[0.157, 0.229]	[0.204, 0.275]
p(RMSEA)[c] $\leq .05$	***	***
	Scaled fit change	
$\Delta\chi^2(\Delta df)$[d]	40.793(3)***	92.147(3)***

Note. Values with superscript letters indicate the initial fixed values taken from Table 4, used to fit the models in Table 5. PTS = Parameter Stability Test; RML = robust maximum likelihood; AIC = Akaike information criterion; CFI = comparative fit index; TLI = Tucker–Lewis index; SRMR = standardized root-mean-square residual; RMSEA = root-mean-square error of approximation; CI = confidence interval. [a] Initial fixed value from model $T1 = 5$. [b] Initial fixed value from model $T1 = 4$. [c] Probability of RMSEA. [d] $\Delta\chi^2$AM = $\Delta\chi^2$ of Asparouhov and Muthén difference.
*** $p < .001$.

the results of the different curves. We observe that from $T1 = 5$ and from $T1 = 4$, the forecast of the values for all the data of $T = 6$ is good, both in their expected values for $T = 6$, and in the CI of the forecasts, being very similar to the original shape.

(iii) To obtain the complete restricted model with the parameters of $T1$, we take the results obtained in Table 6, and copying the values of the shape parameters of the NEXP model, μ_α, $\mu_{\beta 1}$, and b_2, from the analyses of the trimmed samples $T1 = 5$, $T1 = 4$, and $T1 = 3$, so that now those values of the parameters, μ_α, $\mu_{\beta 1}$ and $\mu_{\beta 2}$, are set as input values in the sample for all data, $\boldsymbol{S_{6(T1=5)}}$, $\boldsymbol{S_{6(T1=4)}}$, and $\boldsymbol{S_{6(T1=3)}}$, the results now appear in Table 7.

(iv) In order to verify the structural constancy of the NEXP model, hypothesis $\boldsymbol{S_T = \Sigma(\theta_T)}$, we compare the results with all the data, $T = 6$, with the results of $T1 = 5$; in Table 7, at the bottom, it is verified that $\Delta\chi^2(\Delta df) = 0.326(3)$, with $p = .955$, so the difference between both models is not statistically significant, thus accepting $\boldsymbol{S_{6(T1=5)} = \Sigma(\theta_6)}$, indicating that there is structural stability in the shape parameters of the NEXP function between $T = 6$ and $T1 = 5$. Likewise, we evaluated the structural stability in the NEXP model between $T = 6$ and $T1 = 4$, shown in Table 7 at the bottom, and since $\Delta\chi^2(\Delta df) = 1.079(3)$, $p = .782$, we accept $\boldsymbol{S_{6(T1=4)} = \Sigma(\theta_6)}$; therefore, we accept the structural constancy of the model throw their parameters from $T1 = 4$ to $T = 6$.

Since the NEXP model is internally stable for $T1 = 5$ and for $T1 = 4$, the PCT has also been done for $T1 = 3$. The results appear in the column to the right in Table 7, while in Table 7, we show the results of the projection of $\boldsymbol{S_{6(T1=3)}}$. At the bottom of Table 7, we also display the results of the comparison of $\boldsymbol{S_{6(T1=3)}}$ with $\boldsymbol{\Sigma(\theta_6)}$; the $\boldsymbol{S_{6(T1=3)}}$ with values of 83.400(19), $p < .001$, which when compared with those of $\boldsymbol{\Sigma(\theta_6)}$ results, the $\Delta\chi^2(\Delta df)$ is 17.003(3), $p < .001$, indicate that there is no structural stability from $T1 = 3$ to $T = 6$, where $\boldsymbol{S_{6(T1=3)} \neq \Sigma(\theta_6)}$, despite the fact that in Figure 5C it can be seen that the predicted trajectories for NEXP with $T1 = 4$ are very similar to those for $T = 6$.

Briefly, the NEXP model applied to our data, as shown in Equation 7, demonstrates structural constancy in its shape parameters when comparing $T = 6$ with $T1 = 5$ and $T1 = 4$. However, it lacks constancy when $T1 = 3$. In contrast, the QF model does not exhibit any parameter stability at all.

Interpretation of Parameters

There are authors who propose choosing, among several models, the one with the most easily interpretable coefficients (Cudeck & Harring, 2007; Kaufman, 1996). Therefore, for the QF, we should use the results in Equation 5 and Table 2 for the value of μ_α, or intercept, indicating that the cutoff point of the QF with the Y axis is

Table 6
PST Tests' Main Results for the Negative Exponential Model, in Function of the Trimmed Last Values

Trimming Parameter	$T1 = 5$ ($T2 = 1$) Value (*SE*)	$T1 = 4$ ($T2 = 2$) Value (*SE*)	$T1 = 3$ ($T2 = 3$) Value (*SE*)
	Negative exponential model		
μ_α	−5.738 (1.453)***[a]	−4.528 (1.459)**[b]	−2.782 (1.986)[c]
$\mu_{\beta 1}$	40.738 (1.516)***[a]	40.667 (1.493)***[b]	42.008 (2.936)***[c]
ψ^2_α	135.032 (20.677)***	127.572 (19.695)***	116.795 (20.491)***
$\psi^2_{\beta_1}$	273.301 (30.027)***	292.047 (32.064)***	341.666 (57.749)***
$\psi_{\alpha\beta_1}$	−154.612 (21.30)***	−152.021 (20.733)***	−151.768 (23.626)***
b_2	0.556 (0.039)***[a]	0.506 (0.050)***[b]	0.420 (0.097)***[c]
	Overall fit		
χ^2 (RML)	36.440 (10)***	12.655 (5), $p = .027$	3.179 (1), $p = .075$
Correction factor	1.010	0.917	0.892
AIC	4,324.152	3,531.627	2,724.948
CFI	.958	.983	.991
TLI	.958	.979	.973
SRMR	.088	.070	.045
RMSEA	.137	.104	.124
90% CI	[0.091, 0.186]	[0.033, 0.177]	[0.000, 0.289]
p(RMSEA)[a] $\leq .05$	.002	.091	.126
	Long-run trend		
Y_∞	35.000	36.139	39.226
Level 2 *SE* (Y_∞)	9.955	10.751	12.447
95% CI (Y_∞)	[15.488, 54.512]	[15.068, 57.210]	[14.830, 63.622]

Note. Values with superscript letters indicate the freely estimated values in Table 6 that will be used as the initial fixed values to fit the negative exponential models in Table 7. PTS = Parameter Stability Test; $T1$ = number of waves used; $T2$ = number of waves deleted, being: $T1 + T2 = 6$;; RML = robust maximum likelihood; AIC = Akaike information criterion; CFI = comparative fit index; TLI = Tucker–Lewis index; SRMR = standardized root-mean-square residual; RMSEA = root-mean-square error of approximation; CI = confidence interval.
[a] Model $T1 = 5$. [b] Model $T1 = 4$. [c] Model $T1 = 3$. [d] Probability of RMSEA.
** $p < .01$. *** $p < .001$.

1.123. For the value of $\mu_{\beta 2}$, or t^2 coefficient, −1.017, the negative value indicates that the QF has an inverted U shape, and the small absolute value of $\mu_{\beta 2}$ shows that the inverted U shape is very open, with slow growth and slow decline. For the t coefficient, $\mu_{\beta 1}$, 11.525 indicates that the apex of the QF has shifted to the right, this is, toward the positive end of the X axis. Note also the values of the covariances between them, $\psi_{\alpha\beta_1} = -38.288$, indicating an inverse relationship between the parameters μ_α and $\mu_{\beta 1}$, such that a high value for μ_α for any given participant is normally associated with a low value for $\mu_{\beta 1}$; if $\psi_{\alpha\beta_2} = 3.991$, and $\psi_{\beta_1\beta_2} = -3.310$, this indicates significant shared variance, which adds complexity to the interpretation.

In a NEXP model, the interpretation of the coefficients is more straightforward, so in Equation 11 and Figure 5A, the intercept is −5.190, for $t = 0$. However, this value is meaningless because the values of t start in trial 1, with a value of $Y'_{t=1} = 12.465$; and the LRT, when time trends to infinite, is the sum of μ_α and $\mu_{\beta 1}$, 35.288, so the DV mean expected value with a high value of time, also trends to 35.288. The exponential b_2 value is the shape of the function, with values of b_2 normally showing a very quick increase at the beginning of the function, later an acute curve and finally a stable line trending to $\mu_\alpha + \mu_{\beta 1}$. However, values of b_2 close to zero show a very slow increase, in our case, $b_2 = -0.537$, having a medium-growing arch shape. The negative covariance, $\psi_{\alpha\beta_1}$ indicates that high intercept values, μ_α, correspond to lower values in $\mu_{\beta 1}$ values, and vice versa. Undoubtedly, the NEXP function is less well known than the QF, but its interpretation is much simpler.

Other Polynomial and Nonlinear Models

To check the properties of the NEXP model with other nonlinear models, we have selected only models without inflection point and with a single additional parameter (b_2), in addition to the Level 1 parameters (μ_α and $\mu_{\beta 1}$) of the proposed model: Michaelis–Menten, monomolecular, allometric, and Shinozaki–Kira. In this way, the models analysed here are maintained with the minimum level of mathematical complexity, to facilitate their understanding, in addition to their statistical comparison.

We have tried to fit each of these nonlinear models to our data, and all of them converged except the Michaelis–Menten; the results are shown in Table 8, where we see that the monomolecular model produces the same results (global fit, parameters, and LRT values) as the NEXP model in Table 2; this occurs because in nonlinear models there are some of them that are different reparameterizations of the same model (Bates & Watts, 2007; Konishi, 2014), thereby the NEXP and monomolecular functions are reparameterizations of the same function.

We can observe in Table 8 that the negative allometric and the Shinozaki–Kira models have a somewhat worse overall fit indicators than the NEXP model, since their AIC are bigger (with values exceeding seven points above the NEXP), as are the RMSEA, and have smaller CFI or TLI, and so forth. One detail to consider is that the negative allometric model failed to converge using lavaan, but it successfully converged with Mplus.

We have examined their respective PCTs, and as shown in Table 9 (with the values of the Step (ii) of the PCT for the negative allometric

Table 7

PST Tests' Main Results for the Negative Exponential Model, Imposing the Constrictions of Values μ_α, $\mu_{\beta 1}$, and b_2, Got in Table 6, From $T1 = 5$, $T1 = 4$, and $T1 = 3$, But Applying These Values to All the Sample $T = 6$, Getting the Models With Matrices $S_{6(T1=5)}$, $S_{6(T1=4)}$, and $S_{6(T1=3)}$

Parameter	$S_{6(T1=5)}$ Value (*SE*)	$S_{6(T1=4)}$ Value (*SE*)	$S_{6(T1=3)}$ Value (*SE*)
	Negative exponential model		
μ_α	−5.738[a]	−4.528[b]	−2.782[c]
$\mu_{\beta 1}$	40.738[a]	40.667[b]	42.008[c]
ψ^2_α	131.817 (19.443)***	121.315 (18.338)***	106.793 (16.898)***
$\psi^2_{\beta_1}$	257.314 (26.771)***	247.521 (25.509)***	244.796 (24.836)***
$\psi_{\alpha\beta_1}$	−147.424 (19.574)***	−135.325 (18.394)***	−120.590 (17.228)***
b_2	0.556[a]	0.506[b]	0.420[c]
	Overall fit		
χ^2 (RML)	59.545 (19)***	60.348 (19)***	83.400 (19)***
Correction factor	1.150	1.156	1.167
AIC	5,085.501	5,086.804	5,114.385
CFI	.951	.950	.922
TLI	.961	.961	.939
SRMR	.052	.050	.059
RMSEA	.123	.124	.155
90% CI	[0.088, 0.159]	[0.090, 0.160]	[0.122, 0.190]
p(RMSEA)[d] ≤ .05]	***	***	***
	Scaled fit change[e]		
$\Delta\chi^2(\Delta df)$[f]	0.326(3), $p = .955$	1.079(3), $p = .782$	17.003(3)***

Note. Values with superscript letters indicate the initial fixed values taken from Table 6, used to fit the models in Table 7. PTS = Parameter Stability Test; RML = robust maximum likelihood; AIC = Akaike information criterion; CFI = comparative fit index; TLI = Tucker–Lewis index; SRMR = standardized root-mean-square residual; RMSEA = root-mean-square error of approximation; CI = confidence interval.
[a] Initial fixed value from model $T1 = 5$. [b] Initial fixed value from model $T1 = 4$. [c] Initial fixed value from model $T1 = 3$. [d] Probability of RMSEA. [e] Step (d) of PST test. [f] $\Delta\chi^2$AM = $\Delta\chi^2$ of Asparouhov and Muthén difference.
*** $p < .001$.

model) and on Table 10, Steps (iii) and (iv) of the PCT, the negative allometric model is stable for $T1 = 5$ waves, $\Delta\chi^2(\Delta df) = 1.365(3)$, $p = .714$, but not for $T1 = 4$, $\Delta\chi^2(\Delta df) = 22.882(3)$, $p < .001$.

Similarly, in Table 11 (displaying the values of the Step (ii) of the PCT for the Shinozaki–Kira model) and in Table 12, viewing Steps (iii) and (iv) of the PCT, we see that the Shinozaki–Kira

Table 8

Kanfer and Ackerman's Data ($T = 6$) Main Results in Latent Growth Curve SEM Analysis, Exposing the Main Results of Monomolecular (Equivalent to NEXP), Negative Allometric and Shinozaki–Kira Models

Models Parameter	Monomolecular Value (*SE*)	Negative allometric Value (*SE*)	Shinozaki–Kira Value (*SE*)
μ_α	35.288 (0.955)***	58.363 (7.215)***	43.460 (1.490)***
$\mu_{\beta 1}$	−40.477 (1.495)***	−46.732 (7.253)***	−67.336 (9.000)***
ψ^2_α	95.604 (12.678)***	302.891 (94.158)**	150.189 (20.059)***
$\psi^2_{\beta_1}$	253.110 (27.552)***	336.357 (106.429)**	698.758 (192.912)***
$\psi_{\alpha\beta_1}$	−110.523 (15.449)***	−293.189 (99.254)**	−268.088 (54.881)***
b_2	0.537 (0.035)***	–0.365 (0.075)***	1.116 (0.202)***
	Overall fit		
χ^2 (RML)	60.613 (16)***	72.432 (16)***	67.150 (16)***
Correction factor	1.121	1.122	1.125
AIC	5,090.936	5,104.309	5,098.539
CFI	.946	.932	.938
TLI	.949	.936	.942
SRMR	.050	.054	.052
RMSEA	.141	.158	.151
90% CI	[0.104, 0.179]	[0.122, 0.196]	[0.114, 0.189]
p(RMSEA[a] ≤ .05	***	***	***
	Long-run trend		
Y_∞	35.288	58.363	43.460
Level 2 SE_B (Y_∞)	9.778	17.404	12.255
95% CI (Y_∞)	[15.732, 54.453]	[24.252, 92.474]	[19.440, 67.480]

Note. The Michaelis–Menten model does not converge. SEM = structural equation modeling; NEXP = negative exponential; RML = robust maximum likelihood; AIC = Akaike information criterion; CFI = comparative fit index; TLI = Tucker–Lewis index; SRMR = standardized root-mean-square residual; RMSEA = root-mean-square error of approximation; CI = confidence interval.
[a] Probability of RMSEA.
** $p < .01$. *** $p < .001$.

Table 9
PST Tests' Main Results for the Negative Allometric Model, in Function of the Trimmed Last Values

Trimming Parameter	$T1 = 5$ ($T2 = 1$) Value (*SE*)	$T1 = 4$ ($T2 = 2$) Value (*SE*)
	Negative allometric model	
μ_α	65.971 (12.312)***[a]	183.308 (196.667)[b]
$\mu_{\beta 1}$	−54.339 (12.396)***[a]	−171.676 (196.782)[b]
ψ^2_α	434.497 (205.178)*	4,921.092 (11,483.998)
$\psi^2_{\beta_1}$	483.043 (228.898)*	5,172.903 (11,844.248)
$\psi_{\alpha\beta_1}$	−432.334 (216.176)*	−5,020.562 (11,663.808)***
b_2	−0.306 (0.086)***[a]	−0.086 (0.104)[b]
	Overall fit	
χ^2 (RML)	50.593 (10)***[a]	16.801 (5)**
Correction factor	1.008	.897
AIC	4,338.311	3,535.095
CFI	.935	.973
TLI	.935	.968
SRMR	.092	.068
RMSEA	.170	.129
90% CI	[0.125, 0.217]	[0.065, 0.200]
p(RMSEA)[c] ≤ .05	***	.026
	Long-run trend	
Y_∞	65.971	183.308
SE_B (Y_∞)	20.845	70.150
95% CI (Y_∞)	[25.116, 106.826]	[45.813, 320,803]

Note. Values with superscript letters indicate the freely estimated values in Table 9 that will be used as the initial fixed values to fit the allometric models in Table 10 (Step [ii] of the PST test). $T1$ = number of waves used; $T2$ = number of waves deleted, being: $T1 + T2 = 6$; Step (ii) of the PST test. PST = Parameter Stability Test; RML = robust maximum likelihood; AIC = Akaike information criterion; CFI = comparative fit index; TLI = Tucker–Lewis index; SRMR = standardized root-mean-square residual; RMSEA = root-mean-square error of approximation; CI = confidence interval.
[a] Model $T1 = 5$. [b] Model $T1 = 4$. [c] Probability of RMSEA.
* $p < .05$. ** $p < .01$. *** $p < .001$.

model is also stable for $T1 = 5$, $\Delta\chi^2(\Delta df) = 0.292\,(3)$, $p = .961$, but not for $T1 = 4$, $\Delta\chi^2(\Delta df) = 8.630(3)$, $p = .035$. We can observe that the Shinozaki–Kira model shape of estimated Y' mean values is consistent with the NEXP and the negative allometric models, but there is a technical problem with the Shinozaki–Kira, where the Level 2 $SE_B(Y')$ is very big, and when its 95% CI(Y') is calculated, the interval encompasses to the 100% of the Y' values, so the $SE_B(Y')$ in this data sample, does not have minimum variance.

The NEXP, the negative allometric model and the Shinozaki–Kira models are represented jointly in Figure 6, where it is observed that the NEXP and the negative allometric have very similar Y' profiles from $t = 1$ to $t = 6$, but Y_∞ is higher in the negative allometric than in the NEXP, and the $SE_B(Y_\infty)$ is greater in the negative allometric than in the NEXP. The highest value of $SE_B(Y_\infty)$ is the Shinozaki–Kira model, with the particularity that at the value of $t = 1$ it has the largest $SE_B(Y')$ of all the models and is the only model whose $SE_B(Y_\infty)$ tends to decrease, stabilizing at Y_∞, $SE_B(Y_\infty) = 12.255$ (see Table 8 and Figure 6).

In short, the NEXP model is the best of the models we have analysed so far, both for its internal constancy, verified by the PCT (both for $T1 = 5$ and for $T1 = 4$), its better LRT constancy observed in $T = 6$ ($Y_\infty = 35.558$, 95% CI(Y_∞) [16.393, 54.723]), in $T1 = 5$ ($Y_\infty = 35.000$, 95% CI(Y_∞) [15.488, 54.512]) and in $T1 = 4$ ($Y_\infty = 36.139$, 95% CI(Y_∞) [15.068, 57.210]), showing practically equal profiles for waves from $t = 1$ to $t = 6$ in the data with $T = 6$, $T1 = 5$, and $T1 = 4$ (Figure 5A–5C).

Discussion

In this article, we adapted a parameter structural constancy test that compares the empirical covariance matrix ($\boldsymbol{S}$) with the model-implied covariance matrix [$\boldsymbol{\Sigma(\theta)}$] (Bentler & Satorra, 2010). Unlike traditional PCTs that rely on quadratic error sums (Chow, 1960; Cuthbertson et al., 1992; Hendry, 2011), our approach offers relatively good sensitivity for assessing LGC models, particularly quadratic and exponential forms.

While conventional LGC analyses prioritize overall statistical fit, there has been a notable omission regarding parameter constancy, which refers to the model's ability to remain invariant when shape parameters from individuals' last measurements are removed. We have stressed the description of the QF because it is the most used (and other polynomial models, as straight line, cubic …) in applied research and the more explained in textbooks. By contrast, nonlinear exponential models are rarely used in applied research, and few manuals cover them in depth.

Various authors argue that the selection of a data explanatory model should stem from theoretical frameworks rather than heuristics; however, in most LGC publications, analyses rely on the statistical fit of basic polynomial models such as linear, quadratic, and cubic (Brown et al., 2009; Burant, 2016; Guimond et al., 2022; Livingston et al., 2022; Michel et al., 2021; Reynolds et al., 2005). It is crucial to acknowledge that a good model must also be parsimonious; while polynomial models may appear more

Table 10

PST Tests' Main Results for the Negative Allometric Model, Imposing the Constrictions of Values μ_α, $\mu_{\beta 1}$, and b_2, Got in Table 9, From $T1 = 5$ and $T1 = 4$, but Applying These Values to All the Sample $T = 6$, Getting the Models With Matrices $S_{6(T1\,=\,5)}$ and $S_{6(T1\,=\,4)}$, Step (iii) of PST Test

Parameter	$S_{6(T1=5)}$ Value (*SE*)	$S_{6(T1=4)}$ Value (*SE*)
	Negative allometric model	
μ_α	65.971[a]	183.308[b]
$\mu_{\beta 1}$	−54.339[a]	−171.676[b]
ψ^2_α	395.061 (44.032)***	3,859.823 (395.468)***
$\psi^2_{\beta_1}$	441.160 (45.419)***	4,108.467 (418.325)***
$\psi_{\alpha\beta_1}$	−391.675 (42.027)***	−3,957.710 (403.175)***
b_2	−0.306[a]	−0.086[b]
	Overall fit	
χ^2 (RML)	72.065 (19)***	95.626 (19)***
Correction factor	1.147	1.163
AIC	5,099.668	5,128.201
CFI	.936	.907
TLI	.949	.927
SRMR	.055	.062
RMSEA	.141	.169
90% CI	[0.107, 0.176]	[0.136, 0.204]
p(RMSEA)[c] $\leq .05$	***	***
	Scaled fit change[f]	
$\Delta\chi^2(\Delta df)$[e]	1.365(3), $p = .714$	22.882(3)***

Note. Values with superscript letters indicate the initial fixed values taken from Table 9, used to fit the models in Table 10. PTS = Parameter Stability Test; RML = robust maximum likelihood; AIC = Akaike information criterion; CFI = comparative fit index; TLI = Tucker–Lewis index; SRMR = standardized root-mean-square residual; RMSEA = root-mean-square error of approximation; CI = confidence interval. [a] Initial fixed value from model $T1 = 5$. [b] Initial fixed value from model $T1 = 4$. [c] Probability of RMSEA. [d] $\Delta\chi^2$AM = $\Delta\chi^2$ of Asparouhov and Muthén difference. [e] Step (iv) of the PST test. [f] $\Delta\chi^2$AM = $\Delta\chi^2$ of Asparouhov and Muthén difference.
*** $p < .001$.

parsimonious initially, our findings indicate otherwise. Through our analysis, we have determined that the NEXP model provides superior explanatory capacity, particularly evident in its internal constancy estimated through the PCT, compared to QF models and other nonlinear models with only an additional parameter, such as Michaelis–Menten, allometric, or Shinozaki–Kira.

When comparing QF and NEXP models, we found that the QF model showed acceptable fit only at $T = 6$, but lacked internal constancy when assessed from $T1 = 5$ and $T1 = 4$ to $T = 6$. Conversely, the NEXP model maintained acceptable fit at $T = 6$, with constancy checked by the PCT from $T1 = 5$ and $T1 = 4$ to $T = 6$, making it a more reliable choice for stable trajectory analysis. Other models, like negative allometric and Shinozaki–Kira, were stable only from $T1 = 5$ to $T = 6$. While NEXP emerged as the superior model in this study, it is not universally the best choice for all asymptotically ascending curves without inflection points. Each model should be tested for stability using the PCT. Consider a scenario where a treatment is introduced at $T1 = 4$ within a language development curve. If the researcher incorrectly identifies the curve as QF and analyzes data from $T1 = 5$ to $T = 6$ using a PCT, it might erroneously infer a trend change due to the treatment, as QF parameters would change. In contrast, the NEXP model would show no structural change, avoiding misinterpretation (McCleary et al., 2017; Tan et al., 2012).

Our findings have practical implications, especially regarding sampling strategies. For example, when using the NEXP model, researchers could limit their observations to only $T = 4$ waves, as the model remains valid from $T1 = 4$ and $T1 = 5$ to $T = 6$. In contrast, the QF model changes with each additional wave, lacks internal constancy, increasing resource demands.

The PCT test extends beyond internal fit by identifying the "uniqueness" of the DGP. For example, in the NEXP model, parameters remain consistent across $T1 = 4$, $T1 = 5$, and $T = 6$, indicating high stability. Conversely, the QF model shows parameter variation across these time points, suggesting breakpoints at $T1 = 4$ and $T1 = 5$ relative to $T = 6$, revealing internal instability, and this instability could be mistaken for a significant effect of a therapeutic intervention.

Regarding the use of a piecewise fitting approach in an LGC model, we believe that researchers should aim to identify the underlying DGP. Therefore, piecewise fitting should be considered a last resort. Similarly, when evaluating treatment effectiveness, it is crucial to avoid relying on piecewise adjustments; instead, efforts should focus on identifying the appropriate DGP, from which the correct transfer function can be established.

While we are not claiming that the NEXP model is universally superior, an internal constancy test should be conducted in each case to determine the most stable model based on the sample and results. Ultimately, establishing structural change requires a properly modeled baseline equation with checked internal constancy.

Our study revealed a paradox: fewer measurement waves correspond to better overall statistical fit. For instance, the QF fit is better at $T1 = 4$

Table 11
PTS Tests' Main Results for the Shinozaki–Kira Model, in Function of the Trimmed Last Values

Trimming Parameter	$T1 = 5$ ($T2 = 1$) Value (*SE*)	$T1 = 4$ ($T2 = 2$) Value (*SE*)
	Shinozaki–Kira	
μ_α	44.348 (1.777)***[a]	48.455 (2.948)***[b]
$\mu_{\beta 1}$	−72.361 (11.196)***[a]	−101.227 (21.817)***[b]
ψ^2_α	167.283 (26.590)***	226.161 (41.997)***
$\psi^2_{\beta_1}$	858.577 (283.211)**	1,802.736 (782.891)*
$\psi_{\alpha\beta_1}$	−320.620 (79.756)***	566.079 (178.894)**
b_2	1.212 (0.235)***[a]	1.749 (0.379)***[b]
	Overall fit	
χ^2 (RML)	45.079 (10)***	14.765 (5), $p = .011$
Correction factor	1.013	0.904
AIC	4,332.987	3,533.373
CFI	.944	.978
TLI	.944	.973
SRMR	.091	.069
RMSEA	.158	.118
90% CI	[0.113, 0.206]	[0.051, 0.189]
p(RMSEA)[c] ≤ .05	***	.048
	Long-run trend	
Y_∞	44.348	48.455
Level 2 SE_B (Y_∞)	12.934	15.039
95% CI (Y_∞)	[18.998, 69.698]	[18.979, 77.931]

Note. Values with superscript letters indicate the values (freely estimated) in Table 11 that will be used as the initial fixed values to fit the Shinozaki–Kira models in Table 12. PST = parameter stability test; RML = robust maximum likelihood; AIC = Akaike information criterion; CFI = comparative fit index; TLI = Tucker–Lewis index; SRMR = standardized root-mean-square residual; RMSEA = root-mean-square error of approximation; CI = confidence interval.
[a] From model $T1 = 5$. [b] From model $T1 = 4$. [c] Probability of RMSEA.
* $p < .05$. ** $p < .01$. *** $p < .001$.

than at $T1 = 5$ or $T = 6$, and the NEXP model shows improved fit as $T1$ decreases. Specifically, in the NEXP model, the fit indices are better at $T1 = 3$ (Table 6, last column: AIC = 2,724.948, CFI = .991) compared to $T = 6$ (Table 2, last column: AIC = 5,090.936, CFI = .946), and similar trends are observed for $T1 = 5$ and $T1 = 4$. However, despite excellent fit at $T1 = 3$, imposing the shape parameters from NEXP $T1 = 3$ onto NEXP $T1 = 6$ fails the "contrast hypothesis test," $\Delta\chi^2(\Delta df) = 17.003(3)$, $p < .001$ (Table 7, bottom right), indicating not parameter constancy. In summary, good overall fit does not imply "parameter constancy"; these are distinct concepts, and strong statistical fit should not be mistaken for structural constancy over time.

Regarding parameter interpretation, initial impressions might suggest that the coefficients of a QF would be the most straightforward to interpret. However, this is not the case, possibly influenced by the frequency of encountering QFs. Conversely, the interpretation of an NEXP model or another nonlinear model with an additional parameter (Tables 2 and 3) is notably more straightforward. The NEXP model is defined by fundamental shape parameters such as μ_α, $\mu_{\beta 1}$, and b_2, along with their respective variances and a single covariance term, $\psi_{\alpha\beta_1}$; given its very straightforward shape, μ_α represents the intercept, $\mu_{\beta 1}$ corresponds to the increase from $t = 0$ to the end of the learning or development process, with LRT = $\mu_\alpha + \mu_{\beta 1}$, and b_2 represents the speed of the process. In contrast, the QF model (Tables 2 and 3) includes three shape parameters, μ_α, $\mu_{\beta 1}$, and $\mu_{\beta 2}$, each accompanied by their variances and three additional covariance terms.

Based on our findings, we recommend discarding the QF or the straight line model (the LRT in a straight line is infinite) in longitudinal studies on development or learning, or at least comparing them to other nonlinear models. This comparison should involve contrasting their respective PCT results and overall fit indexes. Despite its historical use as the primary model, particularly in developmental or learning curve analysis, the QF model lacks the fit robustness demonstrated by other nonlinear models.

We have studied a LGC model under "normal conditions" using learning data, akin to developmental data. We recommend conducting a PCT on the normal trajectory before modeling an intervention. In our example, the QF model shows parameter changes from $T1 = 4$ to $T = 6$ and from $T1 = 5$ to $T = 6$. Prima facie, without checking the parameter constancy, these changes might be misattributed to an intervention, creating ambiguity. Additionally, the direction of change must be examined for accurate interpretation. An unstable model is prone to parameter shifts over time, making it difficult to discern whether observed changes stem from the model's instability or the intervention's effects.

This recommendation to model an LGC with internal parameter constancy applies to cases where the LGC includes exogenous IVs or aims to study internal groups through mixture modeling. Without such stability, the effects of the LGC's inherent development could be confounded with those of the IVs or the mixture modeling. We recommend that researchers prioritize models with checked internal constancy, before incorporating exogenous

Table 12

PTS Tests' Main Results for the Shinozaki–Kira Model, Imposing the Constrictions of Values μ_α, $\mu_{\beta 1}$, and b_2, Got in Table 11, From T1 = 5 and T1 = 4, But Applying These Values to All the Sample T = 6, Getting the Models With Matrices $S_{6(T1=5)}$ and $S_{6(T1=4)}$, Step (iii) of PST Test

Parameter	$S_{6(T1=5)}$ Value (*SE*)	$S_{6(T1=4)}$ Value (*SE*)
	Shinozaki–Kira model	
μ_α	44.348[a]	48.455[b]
$\mu_{\beta 1}$	−72.36[a]	−101.227[b]
ψ^2_α	154.451 (18.979)***	181.023 (22.296)***
$\psi^2_{\beta_1}$	789.760 (81.479)***	1,463.968 (149.448)***
$\psi_{\alpha\beta_1}$	−290.865 (34.839)***	−442.419 (51.612)***
b_2	1.212[a]	1.749[b]
	Overall fit	
χ^2 (RML)	66.161 (19)***	77.967 (19)***
Correction factor	1.149	1.160
AIC	5,093.045	5,107.486
CFI	.943	.929
TLI	.955	.944
SRMR	.053	.056
RMSEA	.133	.148
90% CI	[0.099, 0.168]	[0.115, 0.183]
p(RMSEA)[c] ≤ .05	***	***
	Scaled fit change[d]	
$\Delta\chi^2(\Delta df)$[e]	0.292(3), $p = .961$	8.630(3), $p = .035$

Note. Values with superscript letters indicate the initial fixed values taken from Table 11, used to fit the Shinozaki–Kira models in Table 12. PTS = Parameter Stability Test; RML = robust maximum likelihood; AIC = Akaike information criterion; CFI = comparative fit index; TLI = Tucker–Lewis index; SRMR = standardized root-mean-square residual; RMSEA = root-mean-square error of approximation; CI = confidence interval.
[a] Initial fixed value from model $T1 = 5$. [b] Initial fixed value from model $T1 = 4$. [c] Probability of RMSEA. [d] Step (iv) of the PST test. [e] $\Delta\chi^2$AM = $\Delta\chi^2$ Asparouhov and Muthén difference.
*** $p < .001$.

variables or testing interventions. The PCT should be employed systematically to identify models that are both statistically adequate and conceptually aligned with the DGP.

In the adjustment of nonlinear models using only five models (Table 4), we encountered several challenges highlighted in the scientific literature. For instance, some models with the same

Figure 6

Forecasted Values, With Level 2 Upper and Lower at 95% CI Limits, According to the Negative Exponential Model (Continuous Line), Negative Allometric Model (Small Bar Lines and Dots), and Shinozaki–Kira Model (Dotted Line)

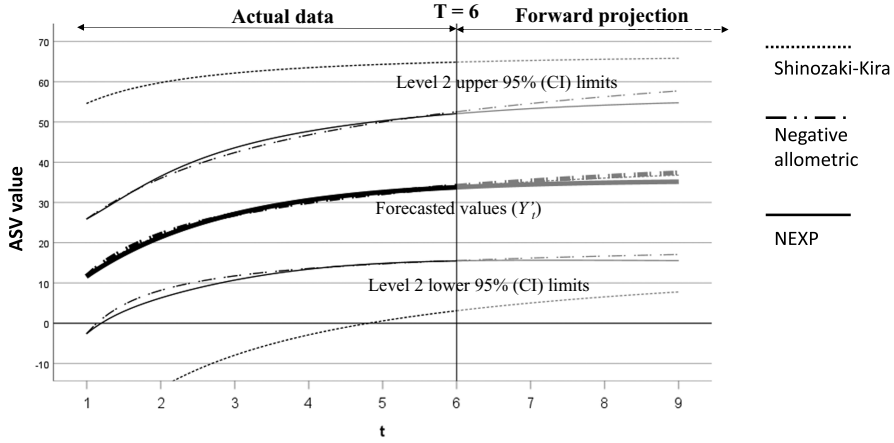

Note. Black lines are waves from 1 to 6, and gray lines are waves from 6 to 9. CI = confidence interval; ASV = Armed Services Vocational Aptitude Battery variable.

complexity index failed to converge (e.g., Michaelis–Menten and logistic function), while others, like the allometric model, converged in Mplus but not in lavaan. Additionally, some models with different names (e.g., monomolecular and NEXP) were mathematically and graphically equivalent. Moreover, graphical differences between nonlinear models were minimal, as shown in Figure 6, where the negative allometric and NEXP models yielded nearly identical values of Y' and 95% CI(Y') of $SE_B(Y')$ from $T = 1$ to $T = 6$. The primary distinction lay in their $SE_B(Y')$ and the parameter constancy (Konishi, 2014; Molenaar & Newell, 1998; Panik, 2014; Preacher & Hancock, 2015; Ratkowsky, 1990; Seber & Wild, 2003).

Determining the minimum $T1$ required for conducting a PCT in LGC modeling remains an open question. Given the absence of a definitive guideline, researchers may inquire about the optimal number of measurement occasions necessary for PCT execution. This consideration stems from the imperative to possess a specific number of degrees of freedom to facilitate the "clipping" of the final data. Our suggestion entails a systematic approach whereby successive values of T (commencing with $T2 = 1$, followed by $T2 = 2$, and so forth) are incrementally eliminated until arriving at a juncture where either the model exhausts its degrees of freedom or exhibits unstable PCT outcomes. This iterative process facilitates the identification of an appropriate threshold for $T1$, thereby ensuring the suitability of subsequent analyses.

In our perspective, LGC models should meet additional criteria beyond those specified by van de Schoot et al. (2017). Firstly, we propose the inclusion of an exploratory figure featuring the total means of each measurement moment and trajectories of randomly chosen individuals from the sample. This visual aid assists in identifying potential inflection points and determining the most suitable group of functions to fit the curve under investigation. Secondly, an evaluation of internal structural constancy is essential, accomplished through techniques like the PCT and comparative analyses with various nonlinear models. These measures serve to elucidate both the geometric and statistical properties inherent in the curves and functions under scrutiny.

This study has limitations that underscore the need for further research: (a) systematic evaluation of parameter constancy across models, including NEXP and QF, is essential to ensure alignment with a valid DGP, using both real-world and simulated data sets; (b) identifying the optimal number of measurement waves ($T1 = T$) required for stable PCT outcomes remains an open question; and (c) Investigating the influence of factors such as ICC, standard errors, and measurement correlations on constancy and fit will further refine model selection. Future research should heed these areas to advance the methodological robustness of LGC analyses.

In summary, advancing LGC methodologies requires moving beyond traditional fit indexes by incorporating PCTs and developing innovative tools for model comparison. Greater training in nonlinear methodologies, combined with enhanced SEM software functionalities, will significantly improve accessibility and application, paving the way for more suitable model analyses.

References

Anselin, L. (1990). Spatial dependence and structural instability in applied regression analysis. *Journal of Regional Science*, *30*(2), 185–207. https://doi.org/10.1111/j.1467-9787.1990.tb00092.x

Aslin, R. N. (1993). The strange attractiveness of dynamic systems to development. In L. B. Smith & E. Thelen (Eds.), *A dynamic systems approach to development: Applications* (pp. 385–400). MIT Press.

Asparouhov, T., & Muthén, B. (2006). *Robust chi square difference testing with mean and variance adjusted test statistics* (Mplus Web Notes No. 10). https://www.statmodel.com/download/webnotes/webnote10.pdf

Asparouhov, T., & Muthén, B. (2010). *Simple second order chi-square correction* (Technical appendix). https://www.statmodel.com/download/WLSMV_new_chi21.pdf

Bai, J., & Perron, P. (2003). Computation and analysis of multiple structural change models. *Journal of Applied Econometrics*, *18*(1), 1–22. https://doi.org/10.1002/jae.659

Baird, S., Jones, N., Hamad, B., Sultan, M., & Yadete, W. (2021). Capturing the complexities of adolescent transitions through a mixed methods longitudinal research design. In P. Banati (Ed.), *Sustainable human development across the life course: Evidence from longitudinal research* (pp. 135–164). Bristol UP.

Bates, D. M., & Watts, D. G. (2007). *Nonlinear regression analysis and its applications*. Wiley.

Bentler, P. M., & Satorra, A. (2010). Testing model nesting and equivalence. *Psychological Methods*, *15*(2), 111–123. https://doi.org/10.1037/a0019625

Berkey, C. S., & Reed, R. B. (1987). A model for describing normal and abnormal growth in early childhood. *Human Biology*, *59*(6), 973–987. https://www.jstor.org/stable/41463961

Bianconcini, S. (2012). Nonlinear and quasi-simplex patterns in latent growth models. *Multivariate Behavioral Research*, *47*(1), 88–114. https://doi.org/10.1080/00273171.2012.640598

Blozis, S. A., Harring, J. R., & Mels, G. (2008). Using LISREL to fit nonlinear latent curve models. *Structural Equation Modeling: A Multidisciplinary Journal*, *15*(2), 346–369. https://doi.org/10.1080/10705510801922639

Bollen, K. A., & Curran, P. J. (2006). *Latent curve models: A structural equation approach*. Wiley.

Brody, S. (1945). *Bioenergetics and growth*. Reinhold.

Brown, E. C., Catalano, R. F., Fleming, C. B., Haggerty, K. P., & Abbott, R. D. (2009). Adolescent substance use outcomes in the raising healthy children project: A two-part latent growth curve analysis. In G. A. Marlatt & K. Witkiewitz (Eds.), *Addictive behaviors: New readings on etiology, prevention, and treatment* (pp. 159–185). American Psychological Association.

Browne, M. W., & Du Toit, S. H. C. (1991). Models for learning data. In L. M. Collins & J. L. Horn (Eds.), *Best methods for the analysis of change: Recent advances, unanswered questions, future directions* (pp. 47–68). APA.

Burant, C. J. (2016). Latent Growth Curve models: Tracking changes over time. *The International Journal of Aging and Human Development*, *82*(4), 336–350. https://doi.org/10.1177/0091415016641692

Burnham, K. P., & Anderson, D. R. (2004). Multimodel inference: Understanding AIC and BIC in model selection. *Sociological Methods & Research*, *33*(2), 261–304. https://doi.org/10.1177/0049124104268644

Burnham, K. P., Anderson, D. R., & Huyvaert, K. P. (2011). AIC Model selection and multimodel inference in behavioral ecology: Some background, observations, and comparisons. *Behavioral Ecology and Sociobiology*, *65*(1), 23–35. https://doi.org/10.1007/s00265-010-1029-6

Campos, J., Ericsson, N. R., & Hendry, D. F. (2005). General-to-specific modeling: An overview and selected bibliography. *International Finance Discussion Papers*. https://www.federalreserve.gov/pubs/ifdp/2005/838/ifdp838.pdf

Chen, D. T., Chan, W., Francis, D. J., Shaywitz, S. E., & Shaywitz, B. A. (2002). Application of two-level negative exponential model to children's learning curve in reading. *Communications in Statistics—Simulation and Computation*, *31*(2), 279–299. https://doi.org/10.1081/SAC-120003339

Cheung, Y. B. (2014). *Statistical analysis of human growth and development*. CRC Press.

Chou, C. P., & Bentler, P. M. (2002). Model modification in structural equation modeling by imposing constraints. *Computational Statistics & Data Analysis*, *41*(2), 271–287. https://doi.org/10.1016/S0167-9473(02)00097-X

Chow, G. C. (1960). Tests of equality between sets of coefficients in two linear regressions. *Econometrica*, *28*(3), 591–605. https://doi.org/10.2307/1910133

Claeskens, G., & Hjort, N. L. (2010). *Model selection and model averaging*. Cambridge UP.

Cole, T. J., Donaldson, M. D., & Ben-Shlomo, Y. (2010). SITAR, a useful instrument for growth curve analysis. *International Journal of Epidemiology*, *39*(6), 1558–1566. https://doi.org/10.1093/ije/dyq115

Collins, L. M. (2006). Analysis of longitudinal data: The integration of theoretical model, temporal design, and statistical model. *Annual Review of Psychology*, *57*(1), 505–528. https://doi.org/10.1146/annurev.psych.57.102904.190146

Cooper, S., Piehl, A. M., Braga, A. A., & Kennedy, D. M. (2003). Testing for structural breaks in the evaluation of programs. *Review of Economics and Statistics*, *85*(3), 550–558. https://doi.org/10.1162/003465303322369713

Cudeck, R., & Harring, J. R. (2007). Analysis of nonlinear patterns of change with random coefficient models. *Annual Review of Psychology*, *58*(1), 615–37. https://doi.org/10.1146/annurev.psych.58.110405.085520

Curran, P. J., Obeidat, K., & Losardo, D. (2010). Twelve frequently asked questions about growth curve modeling. *Journal of Cognition and Development*, *11*(2), 121–136. https://doi.org/10.1080/15248371003699969

Cuthbertson, K., Hall, S. G., & Taylor, M. P. (1992). *Applied econometric techniques*. Harvester Wheatsheaf.

Dao, P. B. (2022). Condition monitoring and fault diagnosis of wind turbines based on structural break detection in SCADA data. *Renewable Energy*, *185*, 641–654. https://doi.org/10.1016/j.renene.2021.12.051

DeMaris, A. (2004). *Regression with social data: Modeling continuous and limited response variables*. Wiley.

Dziak, J. J., Li, R., Tan, X., Shiffman, S., & Shiyko, M. P. (2015). Modeling intensive longitudinal data with mixtures of nonparametric trajectories and time-varying effects. *Psychological Methods*, *20*(4), 444–469. https://doi.org/10.1037/met0000048

Engle, R. F., & Granger, C. W. J. (1987). Cointegration and error correction: Representation, estimation and testing. *Econometrica*, *55*(2), 251–276. https://doi.org/10.2307/1913236

Ferrer, E., Boker, S. M., & Grimm, K. J. (Eds.) (2019). *Longitudinal multivariate psychology*. Routledge.

Ferrer, E., & McArdle, J. (2003). Alternative structural models for multivariate longitudinal data análisis. *Structural Equation Modeling: A Multidisciplinary Journal*, *10*(4), 493–524. https://doi.org/10.1207/S15328007SEM1004_1

Florens, J.-P., & Mouchart, M. (1985). Conditioning in dynamic models. *Journal of Time Series Analysis*, *6*(1), 15–34. https://doi.org/10.1111/j.1467-9892.1985.tb00395.x

Gallant, A. R. (2009). *Nonlinear statistical models*. Wiley.

Geiser, C. (2021). *Longitudinal structural equation modeling with Mplus*. Guilford Press.

Grimm, K. J., & Ram, N. (2009). Nonlinear growth models in Mplus and SAS. *Structural Equation Modeling: A Multidisciplinary Journal*, *16*(4), 676–701. https://doi.org/10.1080/10705510903206055

Grimm, K. J., & Ram, N. (2018). Latent growth and dynamic structural equation models. *Annual Review of Clinical Psychology*, *14*(1), 55–89. https://doi.org/10.1146/annurev-clinpsy-050817-084840

Grimm, K. J., Ram, N., & Estabrook, R. (2017). *Growth modeling. Structural equation and multilevel modeling approaches*. Guilford.

Guimond, A.-J., Trudel-Fitzgerald, C., Boehm, J. K., Qureshi, F., & Kubzansky, L. D. (2022). Is more, better? Relationships of multiple psychological well-being facets with cardiometabolic disease. *Health Psychology*, *41*(1), 32–42. https://doi.org/10.1037/hea0001154

Gujarati, D. N., Porter, D. C., & Gunasekar, S. (2013). *Basic econometrics* (5th ed.). Tata McGraw Hill.

Hansen, B. E. (2001). The new econometrics of structural change: Dating breaks in U.S. labor productivity. *Journal of Economic Perspectives*, *15*(4), 117–128. https://doi.org/10.1257/jep.15.4.117

Harring, J. R., Kohli, N., Silverman, R. D., & Speece, D. L. (2012). A second-order conditionally linear mixed effects model with observed and latent variable covariates. *Structural Equation Modeling: A Multidisciplinary Journal*, *19*(1), 118–136. https://doi.org/10.1080/10705511.2012.634729

Hendry, D. F. (1995). *Dynamic econometrics*. Oxford U.P.

Hendry, D. F. (2011). Revisiting UK consumers' expenditure: Cointegration, breaks and robust forecasts. *Applied Financial Economics*, *21*(1-2), 19–32. https://doi.org/10.1080/09603107.2011.523173

Hendry, D. F., Pagan, A. R., & Sargan, J. D. (1984). Dynamic specification. In Z. Griliches & M. D. Intriligator (Eds.), *Handbook of econometrics* (Vol. 2, pp. 1023–1100). North Holland. https://doi.org/10.1016/S1573-4412(84)02010-9

Hites, R. A. (2019). Break point analyses of human or environmental temporal trends of POPs. *Science of the Total Environment*, *664*, 518–521. https://doi.org/10.1016/j.scitotenv.2019.01.353

Jaccard, J., & Jacoby, J. (2020). *Theory construction and modelbuilding skills: A practical guide for social scientists* (2nd ed.). Guilford.

Jenss, R. M., & Bayley, N. (1937). A mathematical method for studying the growth of a child. *Human Biology*, *9*(4), 556–563. https://www.jstor.org/stable/41447342

Johnson, T. L., & Hancock, G. R. (2019). Time to criterion latent growth models. *Psychological Methods*, *24*(6), 690–707. https://doi.org/10.1037/met0000214

Johnson, W. (2022). Modeling growth curves for epidemiology. In N. Cameron & L. Schell (Eds.), *Human growth and development* (3rd ed., pp. 371–390). Academic Press.

Jöreskog, K. G., & Sörbom, D. (1996). *LISREL 8: User's reference guide*. Scientific Software International.

Kail, R. V., & Ferrer, E. (2007). Processing speed in childhood and adolescence: Longitudinal models for examining developmental change. *Child Development*, *78*(6), 1760–1770. https://doi.org/10.1111/j.1467-8624.2007.01088.x

Kanfer, R., & Ackerman, P. L. (1989). Motivation and cognitive abilities: An integrative/aptitude-treatment interaction approach to skill acquisition. *Journal of Applied Psychology*, *74*(4), 657–690. https://doi.org/10.1037/0021-9010.74.4.657

Kaufman, R. L. (1996). Comparing effects in dichotomous logistic regression: A variety of standardized coefficients. *Social Science Quarterly*, *77*(1), 90–109. https://www.jstor.org/stable/42863433

Konishi, S. (2014). *Introduction to multivariate analysis: Linear and nonlinear modeling*. Chapman and Hall.

Laursen, B. P., Little, T. D., & Card, N. A. (Eds.) (2013). *Handbook of developmental research methods*. Guilford.

Lee, H. B. (2008). Using the Chow test to analyze regression discontinuities. *Tutorials in Quantitative Methods for Psychology*, *4*(2), 46–50. https://doi.org/10.20982/tqmp.04.2.p046

Little, R. J., & Rubin, D. B. (2019). *Statistical analysis with missing data* (2nd ed.). Wiley.

Little, T. D. (2013). *Longitudinal structural equation modeling*. Guilford.

Little, T. D., Preacher, K. J., Selig, J. P., & Card, N. A. (2007). New developments in latent variable panel analyses of longitudinal data. *International Journal of Behavioral Development*, *31*(4), 357–365. https://doi.org/10.1177/0165025407077757

Livingston, N. A., Farmer, S. L., Mahoney, C. T., Marx, B. P., & Keane, T. M. (2022). Longitudinal course of mental health symptoms among veterans with and without cannabis use disorder. *Psychology of Addictive Behaviors*, *36*(2), 131–143. https://doi.org/10.1037/adb0000736

Luitel, H. S., & Mahar, G. J. (2015). A short note on the application of Chow test of structural break in US GDP. *International Business Research*, *8*(10), 112–116. https://doi.org/10.5539/ibr.v8n10p112

Marcoulides, K. M. (2018). Automated latent growth curve model fitting: A segmentation and knot selection approach. *Structural Equation Modeling: A Multidisciplinary Journal*, *25*(5), 687–699. https://doi.org/10.1080/10705511.2018.1424548

Mardia, K. V. (1970). Measures of multivariate skewness and kurtosis with applications. *Biometrika*, *57*(3), 519–530. https://doi.org/10.2307/2334770

McArdle, J. J., & Epstein, D. (1987). Latent growth curves within developmental structural equation models. *Child Development*, *58*(1), 110–133. https://doi.org/10.2307/1130295

McCleary, R., McDowall, D., & Bartos, B. J. (2017). *Design and analysis of time series experiments*. Oxford UP.

McNeish, D., & Dumas, D. (2017). Nonlinear growth models as measurement models: A second-order growth curve model for measuring potential. *Multivariate Behavioral Research*, *52*(1), 61–85. https://doi.org/10.1080/00273171.2016.1253451

Michaelis, L., Menten, M. L., Johnson, K. A., & Goody, R. S. (2011). The original Michaelis constant: translation of the 1913 Michaelis-Menten paper. *Biochemistry*, *50*(39), 8264–8269. https://doi.org/10.1021/bi201284u

Michel, J. S., Rotch, M. A., Carson, J. E., Bowling, N. A., & Shifrin, N. V. (2021). Flattening the Latent Growth Curve? Explaining within-person changes in employee well-being during the COVID-19 pandemic. *Occupational Health Science*, *5*(3), 247–275. https://doi.org/10.1007/s41542-021-00087-4

Molenaar, P. C. M., & Newell, K. M. (Eds.) (1998). *Applications of nonlinear dynamics to developmental process modeling*. Psychology Press.

Muggeo, V. M. R. (2003). Estimating regression models with unknown break-points. *Statistics in Medicine*, *22*(19), 3055–3071. https://doi.org/10.1002/sim.1545

Murayama, K., Pekrun, R., Lichtenfeld, S., & vom Hofe, R. (2013). Predicting long-term growth in students' mathematics achievement: The unique contributions of motivation and cognitive strategies. *Child Development*, *84*(4), 1475–1490. https://doi.org/10.1111/cdev.12036

Muthén, L. K., & Muthén, B. O. (2021). *Mplus v8.6 user's guide* (8th ed.).

Neale, M. C., & McArdle, J. J. (2000). Structured latent growth curves for twin data. *Twin Research*, *3*(3), 165–177. https://doi.org/10.1375/twin.3.3.165

Panik, M. J. (2014). *Growth curve modeling: Theory and applications*. Wiley.

Pavlov, G., Shi, D., & Maydeu-Olivares, A. (2020). Chi-square difference tests for comparing nested models: An evaluation with non-normal data. *Structural Equation Modeling: A Multidisciplinary Journal*, *27*(6), 908–917. https://doi.org/10.1080/10705511.2020.1717957

Pesaran, M. H. (2016). Introduction to dynamic economic modelling. In M. Hashem Pesaran (Eds.), *Time series and panel data econometrics* (Chapter 4, pp. 120–135). Oxford Academic.

Preacher, K. J., & Hancock, G. R. (2015). Meaningful aspects of change as novel random coefficients: A general method for reparameterizing longitudinal models. *Psychological Methods*, *20*(1), 84–101. https://doi.org/10.1037/met0000028

Preacher, K. J., Wichman, A. L., MacCallum, R. C., & Briggs, N. E. (2008). *Latent growth curve modeling*. Sage.

Ratkowsky, D. A. (1990). *Handbook of nonlinear regression models*. Marcel Dekker.

Reynolds, C. A., Finkel, D., McArdle, J. J., Gatz, M., Berg, S., & Pedersen, N. L. (2005). Quantitative genetic analysis of Latent Growth Curve models of cognitive abilities in adulthood. *Developmental Psychology*, *41*(1), 3–16. https://doi.org/10.1037/0012-1649.41.1.3

Rosseel, Y. (2012). Lavaan: An R package for structural equation modeling. *Journal of Statistical Software*, *48*(2), 1–36. https://doi.org/10.18637/jss.v048.i02

Satorra, A., & Bentler, P. M. (2010). Ensuring positiveness of the scaled difference chi-square test statistic. *Psychometrika*, *75*(2), 243–248. https://doi.org/10.1007/s11336-009-9135-y

Seber, G. A. F., & Wild, C. J. (2003). *Nonlinear regression*. Wiley.

Shadish, W. R., Cook, T. D., & Campbell, T. D. (2002). *Experimental and quasi-experimental designs for generalized causal inference*. Houghton Mifflin.

SPSS. (2020). *IBM SPSS statistics 25*.

Stevens, W. L. (1951). Asymptotic regression. *Biometrics*, *7*(3), 247–267. https://doi.org/10.2307/3001809

Tan, X., Shiyko, M. P., Li, R., Li, Y., & Dierker, L. (2012). A time-varying effect model for intensive longitudinal data. *Psychological Methods*, *17*(1), 61–77. https://doi.org/10.1037/a0025814

van de Schoot, R., Sijbrandij, M., Winter, S. D., Depaoli, S., & Vermunt, J. K. (2017). The GRoLTS-Checklist: Guidelines for reporting on latent trajectory studies. *Structural Equation Modeling: A Multidisciplinary Journal*, *24*(3), 451–467. https://doi.org/10.1080/10705511.2016.1247646

Wagner, J., Doehler, S. P., & González, E. (2018). Longitudinal research on the organization of social interaction: Current developments and methodological challenges. In S. P. Doehler, J. Wagner & E. González (Eds.), *Longitudinal studies on the organization of social interaction* (pp. 3–35). Palgrave Macmillan.

Willett, J. B., & Sayer, A. G. (1994). Using covariance structure analysis to detect correlates and predictors of individual change over time. *Psychological Bulletin*, *116*(2), 363–381. https://doi.org/10.1037/0033-2909.116.2.363

Wood, P. K. (2011). Developmental models for children's temperament: Alternatives to chronometric polynomial curves. *Infant and Child Development*, *20*(2), 194–212. https://doi.org/10.1002/icd.692

Wu, W., West, S. G., & Taylor, A. B. (2009). Evaluating model fit for growth curve models: Integration of fit indices from SEM and MLM frameworks. *Psychological Methods*, *14*(3), 183–201. https://doi.org/10.1037/a0015858

Ye, A., & Bollen, K. A. (2022). Can we distinguish between different longitudinal models for estimating nonlinear trajectories? *Structural Equation Modeling: A Multidisciplinary Journal*, *29*(1), 57–69. https://doi.org/10.1080/10705511.2021.1959333

Yuan, K.-H., & Bentler, P. M. (2000). Three likelihood-based methods for mean and covariance structure analysis with nonnormal missing data. In M. E. Sobel & M. P. Becker (Eds.), *Sociological methodology* (pp. 165–200). ASA.

Yuan, K.-H., Lambert, P. L., & Fouladi, R. T. (2004). Mardia's multivariate kurtosis with missing data. *Multivariate Behavioral Research*, *39*(3), 413–437. https://doi.org/10.1207/S15327906MBR3903_2

Received May 29, 2023
Revision received June 5, 2025
Accepted July 7, 2025 ■